NANOPARTICLES OF BIODEGRADABLE POLYMERS FOR DELIVERY OF DIAGNOSTIC/THERAPEUTIC AGENTS: THEIR POTENTIAL APPLICATION IN BRAIN CANCER THERAPY

YU QIANRU

NATIONAL UNIVERSITY OF SINGAPORE

2005

NANOPARTICLES OF BIODEGRADABLE POLYMERS FOR DELIVERY OF DIAGNOSTIC/THERAPEUTIC AGENTS: THEIR POTENTIAL APPLICATION IN BRAIN CANCER THERAPY

YU QIANRU
(B.Eng, Southeast University)

A THESIS SUBMITTED

FOR THE DEGREE OF MASTER OF SCIENCE

GRADUATE PROGRAM IN BIOENGINEERING

NATIONAL UNIVERSITY OF SINGAPORE

2005

Acknowledgement

At the point of finishing my master candidature in Singapore and completing my thesis, I would like to thank the following organizations and people.

Firstly, I would like to thank National University of Singapore and GPBE to give me such a great chance to pursue my research in Singapore. Being exposed to the frontier of bioengineering field, I have thus enriched my knowledge and enhanced my ability for future work.

Secondly, I would like to thank my supervisors, A/P Feng Si-Shen, A/P Wang Shih-Chang, A/P Sheu Fwu-Shan for their useful advice and continuous guidance throughout my graduate study at the department of bioengineering, NUS.

Thirdly, I will thank all my colleagues in Chemotherapeutic Engineering Lab and National University Hospital. I am especially grateful to Ms. Chen Lirong who is my mentor in two lab rotations and Mr Shuter, Borys who kindly helped me with the MRI imaging.

Last but not least, I owe my thanks to my parents and all my friends. Thanks for your help and kind encouragement. You are the most precious treasure all my life.

Table of Contents

Summary

Made up of brain micro-vessel endothelial cells, blood brain barrier (BBB) is a physiologic barrier between the blood and the central nervous system (CNS). It provides neurons with nutrition and isolates the CNS from toxic chemicals in the blood. However, it also severely restricts the delivery of therapeutic agents into the brain. Paclitaxel, one of the most widely used anti-cancer drugs, has limited application in treating brain tumor because of the existence of BBB. Of various strategies developed to enhance drug delivery to the brain, nanoparticles of biodegradable polymers show great potential because they can conquer BBB non-invasively and achieve prolonged pharmacological action of drug molecules.

In this research, paclitaxel loaded poly ($_{D,L}$-lactide-co- glicolide) (PLGA) nanoparticles were fabricated using single emulsion technique. The emphasis was put on the effect of surfactants of nanoparticles. Chemical surfactant polyvinyl alcohol (PVA) and natural surfactants DPPC, vitamin E TPGS were used. Nanoparticles of sizes around 250nm with narrow size distribution and negative surface charge were achieved. Scanning electron microscopy (SEM) and atomic force microscopy (AFM) images showed the morphologies of these nanoparticles. It was found that vitamin E TPGS emulsified nanoparticles had much higher encapsulation efficiency than the other two batches. All batches of nanoparticles had sustained *in vitro* release in about a month. Cell viability study was carried out using rat glioma cell line C6 to test paclitaxel loaded nanoparticles' potential to treat brain tumor. It was found that time

and concentration had effect on the viability.

Cell uptake and confocal laser scanning microscopic studies revealed that fluorescent marker coumarin-6 loaded PLGA nanoparticles were ready to cross the *in vitro* BBB model- Madin-Darby Canine Kidney (MDCK) cell line, but the uptake percentage was affected by surfactants. Particle size effect on cellular uptake was also studied using fluorescent polystyrene nanoparticles with uniform particle sizes. *In vivo* experiment was carried out subsequently. PLGA nanoparticles were overcoated with tween 80 before injecting to the tail vein of the rats. Fluorescence was detected both in rat brain vessels and tissues under fluorescence microscope.

MRI contrast agent Gadolinium-DTPA loaded biodegradable nanoparticles were also developed for future non-invasive *in vivo* imaging. Besides size, morphology, drug entrapment and *in vitro* release study, MRI characteristics of Gd-DTPA encapsulated nanoparticles were also investigated.

Overall, this research conducted systematic investigation on feasibility of nanoparticles of biodegradable polymers for drug delivery across the blood brain barrier. It was found that emulsifiers and particle size played an important part on nanoparticles' ability to cross BBB. Preliminary research on MRI contrast agent Gd-DTPA encapsulated nanoparticles for future non-invasive *in vivo* imaging was also investigated. These results will provide comprehensive information on nanoparticles of biodegradable polymers as potential drug carriers to treat brain cancer and brain related diseases such as AIDS.

Nomenclature

AFM	Atomic Force Microscopy
BBB	Blood brain barrier
CNS	Central nervous system
DCM	Dichloromethane
DMEM	Dulbecco's Modification of Eagle's Medium
DPPC	1,2-dipalmitoyl-sn-glycerol-3-phospatidylchlorine
EE	Encapsulation efficiency
FBS	Fetal Bovine Serum
Gd-DTPA	Gadolinium Diethylenetriaminepenta-acetic Acid
HBSS	Hank's balanced salt solution
HPLC	High performance liquid chromatography
ICP-OES	Inductively Coupled Plasma - Optical Emission Spectrometer
LLS	Laser Light Scattering
MDCK	Madin-Darby Canine Kidney
MDR	Multidrug Resistance
MPEG-PLA	Methoxy poly(ethylene glycol)-poly(lactide)
MRI	Magnetic Resonance Imaging
MRP	Multidrug resistance protein
MTT	3-(4,5-dimethylthiazol-2-yl)-2,5-diphenyltetrazolium bromide
PBS	Phosphate Buffer Saline
P-gp	P-glycoprotein

PLA-PEG	Poly (Lactic acid) - poly(ethylene glycol)
PLGA	Poly ($_{D, L}$-lactide-co-glicolide)
PS	Polystyrene
PVA	Polyvinyl alcohol
SEM	Scanning Electron Microscopy
Vitamin E TPGS	Vitamin E succinate with polyethylene glycol 1000

List of Figures

List of Tables

Chapter 1

Introduction

1.1 Background

Brain cancer is caused by uncontrolled cell growth in the brain. It can be divided into two categories: the primary brain cancer which is originated within the brain and the secondary brain cancer which is originated from cells in other parts of the body and migrate to the brain (oncology channel). Although a lot of efforts have been exerted, brain cancer still remains one of the most difficult diseases to treat mainly because the existence of the blood brain barrier. The blood brain barrier (BBB) is a physiological mechanism that alters the permeability of the brain capillaries so that some substances such as the toxins and drugs are prevented from entering the brain while necessary nutrition is allowed to enter freely. Although BBB plays an important role in maintaining a homeostatic environment for the brain, it also represents a main obstacle for chemotherapy of brain diseases. Paclitaxel, a widely used anticancer drug, has limited application in treating brain tumors because of its poor solubility and BBB permeability. Due to its low solubility, paclitaxel is often administered together with Cremophor EL as a co-solvent which can cause a lot of side effects (Weiss, 1990; Kongshaug, 1991; Dorr, 1994; Fjallskog, 1993). P-glycoprotein, which is abundantly distributed in the BBB, serves as a biochemical barrier and is responsible for paclitaxel's poor brain permeability.

Various carriers have been developed to formulate paclitaxel without the toxic co-solvent (Singla et al., 2002), among which nanoparticles of biodegradable polymers seem to be

an ideal option. However, little information can be found from literature about efficient brain delivery of paclitaxel loaded nanoparticles. On the contrary, nanoparticle formulation for enhanced brain drug delivery often uses water soluble drugs such as darlagin, doxorubicin as model drug due to their poor bioavailability (Schroeder et al., 1998; Gulyaev et al., 1999).

In previous studies, poly(butylcyanoacrylate) (PBCA) was often used as working polymer for enhanced drug delivery to cross the blood brain barrier. However, PBCA is not authorized and may have toxicity effects on CNS (Oliver, et al, 1999; Davis, 2000). Therefore, it is of significance to choose a polymer with more favorable properties to develop nanoparticles. Poly ($_{D,L}$-lactide-co-glycolide) (PLGA), a widely used biodegradable polymer which has been approved by Food and Drug Administration (FDA), is a good candidate. Due to its unique advantages over other polymers such as biodegradability, biocompatibility and ability for sustained release, PLGA has been broadly applied in drug delivery.

Apart from the nature of polymers, proper surfactant and particle size are two important factors that can affect nanoparticles' fate both *in vitro* and *in vivo*. It was found that nanoparticles overcoated with some chemical surfactants such as poloxamer 407, poloxamer 188 and polysorbate 80 could yield much higher uptake by bovine brain microvessel endothelial cells (Borchard et al, 1994). Researchers also found that particle size could significantly affect cellular and tissue uptake. The uptake efficiency of nanoparticles was much higher than that of microparticles (Panyam and Labhasetwar,

2003). However, very limited studies have been carried out for the application of natural surfactant and particle size effect on brain delivery.

When *in vivo* experiments are carried out to evaluate drug delivery to the brain, indirect or invasive methods such as the hot-plate test, tail-flick test and fluorescent brain slice are often adopted (Kreuter et al., 1995; Ramge et al., 1999; Sun et al., 2003). These methods help us to know the efficiency of drug carriers *in vivo* qualitatively. However, the specific delivery site can not be assessed readily. As a high contrast imaging instrument, magnetic resonance imaging (MRI) is very useful in medical field. Contrast agent such as iron oxide and gadolinium-DTPA can be used to enhance the imaging significantly. By encapsulating MRI contrast agent into the nanoparticles, it is possible to visualize the exact site of nanoparticles *in vivo* with a noninvasive way. Up to now, only two very recent papers presented similar ideas of using Gd-DTPA encapsulated microparticles for bladder imaging (Faranesh et al., 2004; Chen et al., 2005). No literature has been found about using positive contrast agent Gd-DTPA loaded nanoparticles for brain imaging.

1.2 Objectives

A series of experiments will be carried out to investigate the feasibility of PLGA nanoparticles to cross the BBB both *in vitro* and *in vivo*. The research will be focused on surfactant coating technique and particle size effect. The potential for treating brain cancers with therapeutic agent paclitaxel loaded PLGA nanoparticles will also be investigated by cell line experiment. Besides, MRI contrast agent Gd-DTPA loaded nanoparticles of biodegradable polymers are also developed for future investigation of non-invasive imaging of nanoparticles *in vivo*.

In the therapeutic agent/fluorescence loaded nanoparticles study, paclitaxel or fluorescent marker coumarin-6 loaded PLGA nanoparticles will be fabricated using the extraction/evaporation method. Two natural surfactants: vitamin E TPGS and DPPC (1,2-dipalmitoyl-sn-glycerol-3-phospatidylchlorine) will be tried as novel emulsifiers and surface coating during the fabrication process compared with traditional emulsifier PVA (polyvinyl alcohol). Particle size and size distribution will be measured with the laser light scattering (LLS) system. Surface charge will be determined by the zeta potential analyzer. Scanning electron microscopy (SEM) and atomic force microscopy (AFM) allow us to get a close look at the particle morphology. Encapsulation efficiency and *in vitro* release of paclitaxel from the nanoapheres are measured by the high performance liquid chromatography (HPLC). MDCK (Madin-Darby canine kidney) cell line will be used as a simple *in vitro* BBB model for uptake study of fluorescence loaded PLGA nanoparticles. Direct evidence of cellular uptake of nanoparticles will be presented by confocal study. Particle size effect will also be detected by MDCK cell uptake experiment using commercially available fluorescent polystyrene nanoparticles with uniform particle sizes. The potential for drug loaded PLGA nanoparticles to treat brain tumors will be verified by cell viability study using MTT assay with rat brain tumor cell line C6 as the model. Finally, preliminary *in vivo* study will also be carried out by observing brain tissue slice under fluorescence microscopy after injection of fluorescence loaded PLGA nanoparticles to the rats.

In the MRI contrast agent loaded nanoparticles study, Gd-DTPA loaded nanoparticles of biodegradable polymers such as PLGA and MPEG-PLA will be developed with different fabrication methods. The achieved nanoparticles with favorable properties will be

characterized by LLS, zeta potential analyzer and SEM. Inductively coupled plasma - optical emission spectrometer (ICP-OES) will be used to measure drug entrapment and *in vitro* release profiles. MRI characteristics of the contrast agent loaded nanoparticles will also be investigated.

1.3 Thesis Organization

The body of this thesis is made up of seven chapters. Chapter 1 gives a brief introduction to the project. It comprises of the general background as well as the objectives of the proposed project. Chapter 2 is literature review on brain cancer, blood brain barrier, paclitaxel and various technologies to fabricate nanoparticles. Known research on nanoparticles to enhance CNS drug delivery will also be described in this chapter. In chapter 3, the materials and methods used in all experiments are recorded. The experimental results and discussions are presented in chapter 4 and chapter 5. In chapter 4 and 5, we present the results of applying paclitaxel and fluorescence marker loaded nanoparticles of biodegradable polymers respectively for treating brain cancer cells and enhancing brain drug delivery. In chapter 6, we develop novel MRI contrast agent loaded nanoparticles for imaging purpose. Conclusion drawn from the project and recommendations for future work are presented in chapter 7.

Chapter 2

Literature Review

2.1 Paclitaxel and Its Limitations in Modern Chemotherapy

Discovered in 1971(Wani et al., 1971) and first approved by US FDA in 1992 for treatment of ovarian cancer, paclitaxel becomes one of the most promising anti-cancer drugs that can deal with a wide spectrum of cancers such as ovarian, breast and non-small cell lung cancers. It also has application in treating brain related diseases like AIDS (Feng & Shu, 2003; Lopes et al., 1993; Donehower et al., 1987; Panchagnula, 1998). Paclitaxel exerts its effect by blocking the replication of cancer cells in the late G2-mitotic phase. The interaction between paclitaxel and cells makes microtubules dysfunctional and leads to apoptosis of cancer cells (Horwitz, 1992).

Despite the effectiveness of paclitaxel in chemotherapy, it also has quite a few limitations. These are also limitations in current chemotherapy. The reasons mainly lie in the following four aspects:

(1) *Availability*. Paclitaxel was extracted from the bark of very slow-growing west yew with low extraction rate (<0.04%) (Cragg, 1991). In order to solve the problem, alternative sources for preparation of semi-synthetic taxol and taxol analogues have been found, such as needles and twigs of English yew trees or Chinese red bean yew trees. Unlike the bark, the needles can regenerate and provide a continuous source for production (Horwitz, 1992). However, efficient

and low-cost ways of large-scale synthesis of paclitaxel still remains a challenge.

(2) *Dosage form and toxicity*. In 1971, Wall and his colleagues first reported the structure of taxol and its cytotoxicity to KB cell line and mouse leukemia cells (Wani, 1971). It is obvious that paclitaxel has some benzene rings and other hydrophobic structures (refer to Fig 2.1 below), which lead to its low water solubility of less than 0.5mg/L. There is no way for direct injection of paclitaxel by dissolving it in distilled water, the only dosage form available in clinical administration uses Cremophor EL and dehydrated alcohol as adjuvant, which is rather toxic and can cause serious side effects such as hypersensitivity reaction, neurotoxicity, cardiotoxicity and nephrotoxicity (Weiss, 1990; Kongshaug, 1991; Dorr, 1994; Fjallskog, 1993).

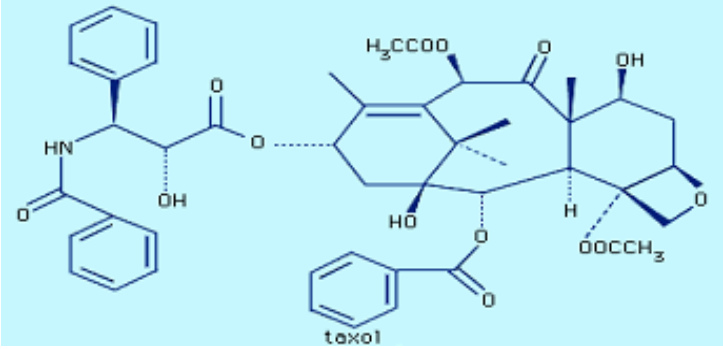

Fig 2.1 Chemical structure of paclitaxel

(3) *Drug Resistance and bioavailability.* It has been found that paclitaxel is able to induce the multidrug resistance (MDR) phenotype with overexpression of P-glycoprotein (P-gp) (Horwitz, 1992; Roy & Horwitz, 1985; Greenberger et al., 1987; Drion et al., 1996). P-gp exists in the cell membrane and serves as a kind of efflux pump that can prevent drugs and other toxic substances from entering cells

(Gatmaitan & Arias, 1993). P-gp is widely distributed in many tissues, such as gastro-intestinal tract, kidney and blood brain barrier. It has already been found that paclitaxel has a rather high affinity for P-gp transporter. Another problem is when drugs are administered, especially orally, they have to withstand metabolic barriers before reaching the blood system. There are a lot of digestive enzymes throughout the GI tract which can degrade drugs and further result in a low bioavailability.

(4) *Targeted and controlled release.* Although paclitaxel has excellent effect on tumor cells, it can also harm normal cells, especially cells that divide quickly such as the bone marrow and lining of the GI tract. Many dangerous side effects may be caused by this kind of non-specific action, such as loss of hair, fussy thinking and difficult concentrating. Another problem is that in order to achieve therapeutic effect, drug concentration should be between the therapeutic level, i.e., above the minimum effective level but below the toxic level. Thus the initial burst should be lowered to achieve a prolonged and sustained release. Besides, drugs may be cell-cycle or cell-growth-phase specific. Thus, cell-cycle specific drugs can be developed to achieve maximum effect (Ratain et al., 1990). Briefly, the desired pharmacokinetics is to release a sufficient quantity of drugs at the right time, the correct location and over a long period of time.

2.2 Brain Cancers and Blood Brain Barrier (BBB)

2.2.1 Brain Cancers and Cancer Treatment

Cancer is a group of diseases characterized by uncontrolled cell division leading to

growth of abnormal tissues. Cancer can spread from its original site to other parts of the body and can be fatal (Web definitions for cancer). Every year, more than 10 million people are diagnosed with cancer and 6 million people die of cancer, which accounts for 12% of deaths worldwide. Although brain cancers are rare cancers which represent only 1.5% of all cancers, the death rate of brain cancers is very high. Moreover, brain cancer also ranks second in all childhood cancers, representing 21% of childhood cancer cases (American Cancer Society). There are basically two kinds of brain tumors. One is primary brain tumors which start in the brain, the other is metastatic brain tumors which are cancers from other parts of the body that can spread to the brain and cause secondary tumor through a process called metastasis. The cells of a metastatic brain tumor resemble the cells of the organ where the tumor startes, not brain cells.

Like other cancers, effective treatments of brain cancers include surgery, radiotherapy, chemotherapy, hormone therapy, biotherapy, and immunotherapy (Oncology, 2002). Two or more methods are often used in combination to achieve better effects. Surgery is the primary method for treatment of brain tumors that can be removed without damaging critical neurological functions. Radiation therapy and chemotherapy are often combined with surgery as secondary and adjuvant treatment. However, severe side effects often accompany these treatments. One of the most important factors that limit brain cancer chemotherapy is due to the existence of the blood brain barrier.

2.2.2 Introduction to the Blood Brain Barrier

2.2.2.1 History of Blood Brain Barrier

The concept of blood brain barrier was first raised by the German scientist Paul Ehrlich in 1885(Enrlich, 1885). After that, many studies have been carried out on this important physiologic barrier. Table 2.1 gives a brief summary of the research history on BBB.

Table 2.1 Summary of BBB History

Discoverer	Time	Main Point
Ehrlich P	1885	i.v. injection of acidic vital dyes stain all rabbits body except brain and spinal cord (Enrlich, 1885)
Lewandowsky	1900	coin the term blood-brain barrier while studying potassium ferrocyannide penetration into the brain (BBB history)
Goldmann EE	1909	i.v. injection of trypan blue to cerebrospinal fluid stains entire brain but not the internal organs(Goldmann, 1909)
Gautier& Stern	1920s	bile salt, morphine and bromide appear in CSF while bile pigment, epinephrine and curare not after i.v. injection
Broman	1941	tight junction not the astrocytic end forms barrier function of BBB (BBB history)
Reese& Karnovsky Reese et al.	1967 1970	visulize BBB using electron microscope & traceable proteins, revealing the protein diffuse past astrocytic end feet and stop at tight junction (Reese & karnovsky, 1967; Reese et al., 1970)
Weiler-Guttler	1989	characteristics of BBB; studies in molecular biology of BBB, cloning and sequencing glucose transporter gene (weiler-Guttler et al., 1989)
Muldoon LL	1999	BBB is a physiologic barrier (Muldoon et al., 1999)

2.2.2.2 Structure and Function of the Blood Brain Barrier

The blood brain barrier is created by tight apposition of endothelial cells lining blood vessels in the brain and is surrounded by astrocyte foot process. A thin basement membrane surrounds the endothelial cells and associated pericytes, providing mechanical support as well as a barrier function. The part in the circle in Fig 2.2 is the BBB site.

There are quite a few important differences between the ultrastructure of brain blood vessels and systemic blood vessels. The brain capillaries lack fenestration that exists in

other systemic capillaries, instead, the membrane of the endothelial cells in the brain is fused into tight junctions, forming continuous, uninterrupted structures. These endothelial tight junctions are the anatomical site of BBB and play an important role in preventing the free exchange of substances between blood and brain (Brightman & Reese, 1969; Reese et al., 1970).The tight junctions result in a much higher transendothelial electrical resistance than other tissues (>50 times), which makes the BBB more hydrophobic and reduces the aqueous based paracellular transport (Lo et al., 2001). BBB also possesses specific enzyme systems, glucose transporters and protein receptors, which indicates its special mechanisms in exchanging substances. Moreover, blood brain barrier is incorporated with many efflux proteins such as P-glycoprotein (P-gp), multidrug resistance protein (MRP). These proteins are responsible for ATP-dependent outward transport of a wide range of substances, including many therapeutic agents (Crone, 1971).

The major function of the blood brain barrier is to protect the brain from possible toxins while supply it with necessary nutrients. Thus it acts both as an impermeable wall and a selective sieve (Betz, 1992). Due to its special structures mentioned above, blood brain barrier effectively filters most ionized, water-soluble molecules greater than 180 Daltons and substances that are substrates of its efflux system. Only small, lipophilic molecules can cross the BBB (Lee,2001;Kroll& Neuwelt, 1998). Several mechanisms are known to be involved in the transport of substances across BBB. Only a few substances such as water can enter the brain using the paracellular route because of the existence of the tight junction. Lipophilic molecules can cross BBB by simple diffusion through transcellular pathway. Lipophilicity and hydrogen bonding potential determine the ability of molecules to cross BBB (Egleton& Davis, 1997). However, a large family of lipid soluble

substances is also substrates of efflux P-gp system thus results in poor brain uptake (Tamai& Tsuji, 2000). BBB's selectivity also indicates that a specific carrier system exists to transport small polar solutes such as glucose (Begley, 1996). Carrier mediated transport in BBB is a major system for endogenous substances and nutrients to enter the brain. Finally, endocytic mechanisms, whether specific or adsorptive, are responsible for the transport of large proteins and peptides across BBB.

2.2.2.3 *In Vitro* and *In Vivo* Models of Blood Brain Barrier

(a) *In Vitro* BBB Models

In vitro BBB models can only represent part of the properties of *in vivo* BBB and they share some basic characteristics. Currently, three types of brain capillary endothelial cell culture are essentially in use: primary cultures, cell line and co-culture systems.

Isolated brain capillaries represent the first developed and closest to *in vivo* system of *in vitro* BBB models (Joo, 1992; Pardridge, 1998). The system next closest is primary brain endothelial cells (BEC) isolated from or grow out of brain capillary fragment. However, due to the difficulty to prepare primary BEC, a number of immortalized cells have been developed to act as *in vitro* BBB model. At present, there are more than 15 different cell line models, including immortalized bovine BEC lines, porcine BEC lines, murine cell lines, primary rat BECs and human cell lines (Durieu et al., 1991; Teifel and Friedl, 1996; Wijsman and Shievers ,1998; Mooradian and Diglio, 1991; Muruganandam et al.,1997). The last *in vitro* BBB model is the co-culture system which consists of a co-culture of brain capillary endothelial cells on one side of a filter and astrocytes on the other. The

strong correlation between this model and *in vivo* situation demonstrates it an important tool for studying the drug delivery to the blood brain barrier (Dehauck et.al., 2000).

(b) In Vivo Techniques

The most common techniques for *in vivo* study of blood brain barrier include the intravenous injection method, the brain efflux index (BEI), the brain perfusion and the micro-dialysis. Table 2.2 below gives a brief summary of these methods.

Table 2.2 Summary of *in vivo* techniques to study BBB

Methods	Description
i.v. injection	"gold standard" for all BBB work; inject solute intravenously, determine solute concentration in brain, plasma and CSF at different times; system intact, reflect true *in vivo* situation; complexity often affects data. Representative work: Ehlich, 1885
brain efflux index	defined as "amount of drug effluxed at BBB" over "amount of drug injected into the brain"; involve direct microinjection of test solute and reference tracers into the brain; can be used to investigate mechanisms of brain-to-blood efflux. Representative work: Kakee et al., 1996
in situ brain perfusion	replace circulation to brain via direct infusion of saline with solute of known concentration to the brain or major vessels for a known interval, perfusion is stopped at set time and amount of solute in brain is determined; relative simple to study kinetics of brain uptake, transport or permeability constants. Representative work: Takasato et al., 1984; Smith, 1996
micro-dialysis	physiological perfusate is pumped through the semi-permeable microdialysis probes in CNS, compounds in extracellular fluid diffuse into perfusate and their concentration can be measured by HPLC, thus tissue concentration of solutes can be measured; quantitatively determine transport across BBB and brain influx and efflux kinetics; invasive, can cause dysfunction of BBB. Representative work: Wang & Welty, 1996

2.2.2.4 Strategies to Conquer the Blood Brain Barrier

While the characteristics of blood brain barrier provide a formidable obstacle for drug delivery to CNS, it is not insurmountable. A variety of strategies have been developed to enhance drug delivery to the brain (Misra et.al., 2003). They can mainly be divided in two categories: BBB manipulation and drug manipulation.

(a) BBB Manipulation

Methods that belong to the BBB manipulation include: osmotic disruption of BBB, biochemical methods to open BBB and alternative routes to overcome BBB.

Rapoport et al. demonstrated that intracarotid injection of inert hypertonic solutions such as arabinose would artificially create osmotic pressure and resulted in more than 20 folds increase in brain concentration of hydrophilic drugs (Rapoport et.al., 1978). In contrast to osmotic disruption of BBB, biochemical methods can selectively open brain tumor capillaries and are potentially safer. Sanovich et al. discovered increased permeability of BBB to lanthanum due to the administration of the bradykinin analog RMP-7 (Sanovich et al., 1995). However, disruption of BBB will cause unexpected damage to the brain such as entering of toxins, abnormal neuronal functions and altered glucose uptake (Miller, 2002). The last method is to develop methodologies not relying on the cardiovascular system, thus bypass BBB altogether. Alternative routes include intraventricular, intrathecal, olfactory route and direct brain interstitial delivery (Misra et al., 2003). Slow rate of drug distribution, clinical incidence of hemorrhage and CNS

infection, active nasal enzyme activity need to be overcome in further investigation of this method.

(b) Drug Manipulation

Drug manipulation includes prodrug, lipophilic analogs, chemical drug delivery, carrier mediated drug delivery and receptor/vector mediated drug delivery. Prodrug is pharmacologically inactive compounds by modification of the parent drug. After administration, prodrug comes to site of action more readily and maintains for a longer time due to its own characteristics; the drug will then convert to its active form to take effect by a single activating step. Lipophilic analogs allow drugs to become more lipid soluble, thus can increase its ability to cross the BBB. One example of this is the liposome. PEGylated immuno-liposomes can cross the BBB *in vivo* through receptor mediated transport (Huwyler et. al., 1997). Chemical drug delivery is to target active biologic molecules to certain sites based on predictable enzyme activation. Carrier, receptor and vector mediated drug delivery to the brain brings in the chimeric peptide technology, where non-transportable drugs such as peptide are conjugated to a BBB transport vectors. Nanoparticles have become one of the most popular and promising vectors for drug transportation across the blood brain barrier (Kreuter et. al., 1995; Peppas and Blanchette, 2004).

2.3 Nanoparticles of Biodegradable Polymers for Drug Delivery

Nanoparticles are colloidal particles of sizes ranging from 1nm to 1000nm. Drugs are dissolved, entrapped or encapsulated in the particles (Lockman et al., 2002). The use of

nanoparticles for drug delivery offers several advantages which include improved bioavailability through sustained release, protection of drugs from degradation and premature inactivation, reduced toxicity to normal cells through targeted delivery by surface modifications of the nanoparticles and increased ability to conquer the P-glycoprotein through masking the drug from being recognized by P-gp. There has been wide research on nanoparticles of biodegradable polymers for drug delivery.

2.3.1 Basic Information of Biodegradable Polymers

Biodegradable polymers are widely used for drug delivery and controlled release because they eliminate the need of removing delivery systems after administration. Drugs are released from polymer matrix by diffusion, polymer degradation or erosion. Various kinds of biodegradable polymers have been developed and summarized in table 2.3 (Uhrich et.al., 1999).

Table 2.3 Summary of biodegradable polymers for drug delivery

Type	**Description& Representative Polymers**
Biopolymers	natural polymers, especially poly(saccharide) family, such as starch, cellulose, chitosan.
Poly(esters)	best studied biodegradable system with product in clinical use; can be synthesized using ring-opening polymerization; representative polymers include poly(lactic acid), poly (glycolic acid) and their copolymers, poly (ethylene glycol) block copolymers.
Poly(ortho esters)	allow release of drugs after polymer chain hydrolysis, research on this polymer focuses on adding polyols to diketene acetals such as 3,9-diethylidene-2,4,8,10-tetraoxaspiro[5.5] undecane(DETOSU)
Poly(anhydrides)	allow heterogeneous erosion and mainly undergo surface erosion; prepared by melt-condensation polymerization; representative polymers are based on *p*-(carboxyphenoxy) propane (CPP), sebacic acid (SA) and *p*-(carboxyphenoxy) hexane (CPH).

Poly(amides)	amino acid-derived polymers, mainly deliver low molecular weight drugs; degradation rate depends on hydrophilicity of amino acid; representative polymers include poly(lactic acid-*co*-lysine) (PLAL).
Phosphorus-Containing Polymer	can perform substitution reactions; have unique inorganic P-N backbones; representative polymers include poly(phosphazenes) and poly(phosphoesters).

Among all the biodegradable polymers used for drug delivery, poly(lactic acid-*co*-glycolic acid) (PLGA) and poly(ethylene glycol) (PEG) block copolymers receive wide attention and investigation. Both of them are FDA approved polymers and have been used in clinical trials (Beck et. al., 1983). They are especially broadly used in fabricating micro and nano spheres as drug carriers for controlled release. Fig 2.2 below shows the chemical structures of PLA, PLGA, PEG and PEG included diblock copolymer MPEG-PLA.

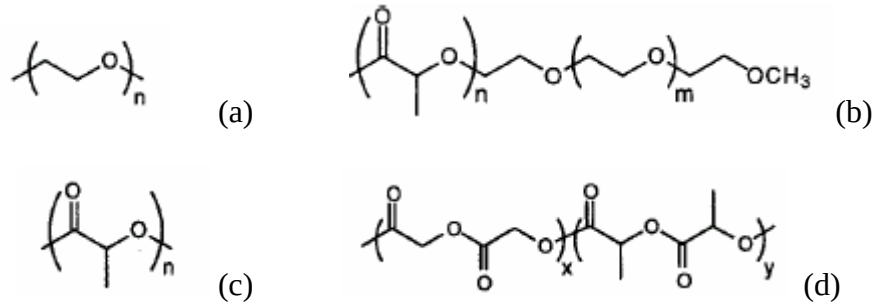

Fig 2.2 Chemical structures of PEG(a), MPEG-PLA(b), PLA(c) and PLGA(d)

PLGA is the copolymers of lactic and glycolic acid (PLA and PGA). It has faster degradation rate than that of PLA and its degradation products are natural metabolites (Leong and Langer, 1987). The degradation rate of PLGA varies within months with different L:G ratios. Release from PLGA microcapsules and microspheres has been emphasized since steroids have low permeability in PLGA (Beck et.al., 1983). It is

suggested that the release kinetics of the microparticles are initial diffusion plus a later combined erosion and diffusion (Leong and Langer, 1987).

PEG and its high molecular weight form PEO (poly(ethylene oxide)) have very good biocompatibility. Due to its hydrophilic nature, PEG also has good protein resistivity (Kwon and Kataoka, 1995; Torchilin and Papisov, 1994). Proteins will have longer circulation time and avoid being taken up by the RES system in the body by attaching PEG chains to the surface of them. Many groups also have a deep investigation on PEG block copolymers. Methoxy poly(ethylene glycol)-poly(lactide acid) (MPEG-PLA) is the diblock copolymer of PLA and methoxy PEG. MPEG-PLA possesses amphiphilic structures thus have surfactant properties. The inclusion of PEG into copolymers will help them to have more favorable properties to be used as drug carriers. For example, MPEG-PLA nanoparticles have more blood circulation time than that of PLA nanoparticles *in vivo* (Gref et al., 1994). Other PEG block copolymers such as triblock PLA-PEG-PLA and multi-block copolymer of L-lactide and ethylene oxide have also been developed (Uhrich et al.,1999).

2.3.2 Manufacture Techniques of Nanoparticles

Various methods have been developed to fabricate nanoparticles. Basically, they are either by dispersing preformed polymers or by polymerizing monomers (Feng and Chien, 2003). Some common methods for fabricating nanoparticles are summarized below.

(1) *Solvent evaporation/extraction process*. This method includes single emulsion and double (multiple) emulsion. Single emulsion, which is also referred to as oil-in-water

(o/w) method, is often used to encapsulate hydrophobic drugs. Briefly, the preformed polymer and drug are dissolved or dispersed in a water immiscible organic solvent such as dichloromethane (DCM) and chloroform. After sonication, the organic phase is slowly poured into water phase containing amphiphilic emulsifiers. The mixture then undergoes high-speed homogenization. Then the organic phase is evaporated or extracted before centrifuging to remove the excess emulsifiers. The final product is obtained by drying the emulsion under suitable conditions. For encapsulating hydrophilic drugs such as proteins and peptides, double emulsion (water-in-oil-in-water) is often used. This method is most similar to that of single emulsion except that the aqueous solution of the drug is added to the polymer contained organic solvent with sonication to form the first w/o emulsion before putting that into the water phase (Jain, 2000).

(2) *Spontaneous emulsification/solvent diffusion process*. This method is sometimes referred to as the nanoprecipitation method. Polymer and drug (either hydrophobic or hydrophilic) are dissolved or dispersed in a mixture of water soluble organic solvent such as acetone and water-insoluble solvent such as DCM. Then the organic phase is added to the aqueous phase drop by drop. Nanoparticles are formed at the same time. The spontaneous diffusion of water-soluble solvent creates an interfacial turbulence between oil and water phase leading to the formation of smaller particles (Dong and Feng, 2004).

(3) *Spray Drying*. Spray drying is a fast and convenient method suitable for mass production. It is appropriate for both hydrophilic and hydrophobic drugs and less dependent on polymer species (Wagenaar and Muller, 1994). Briefly, drugs are suspended or dissolved in organic solution where polymer is also dissolved. Then the mixture is

spray dried to produce particles.

(4) *Phase separation method (coacervation)*. This method is applicable to both hydrophilic and hydrophobic drugs. Briefly, polymer is dissolved in an organic solvent before the drug is dissolved or dispersed in it. Then an organic nonsolvent is added to the above system with stirring to extract the polymer solvent. Due to the phase separation, the polymer forms soft coacervate droplets entrapping the drug. Then the system is transferred to another organic nonsolvent of large amount to harden the particles and form final product (Jain, 2000).

(5) *Polymerization of monomers*. Polymerization includes emulsion polymerization and interfacial polymerization. Emulsion polymerization builds up a chain of polymers from single monomers. The process initiates by radical or ion formation and residual monomer is removed by filtration. The finally formed nanoparticles can act as drug carriers by drug adsorption. Interfacial polymerization happens when monomer-contained organic phase and aqueous phase are brought together by mechanical force. This process can encapsulate drugs by adding them with monomer in the organic phase (Couvreur et al., 1979; Lockman et al, 2002).

Other methods include salting out, superficial fluid spraying, solid lipid nanoparticles etc. Polymer type, co-polymer ratio, drug loading level, mechanical strength level, emulsifiers added, temperature, pH, molecular weight etc. exert effect together to determine the characteristics of nanoparticles (Feng and Chien, 2003).

2.3.3 Current Research on Biodegradable Nanoparticles across BBB

Of so many strategies discussed previously to conquer the blood brain barrier and treat brain tumors, nanoparticles seem to be a strong candidate due to their biocompatibility, possibility for sustained release and ability to mask the P-gp efflux system. Lockman et al. summarized the ideal properties of polymeric nanoparticles across the BBB, which includes: nontoxic, biodegradable/biocompatible of the polymers; nonthrombogenic and nonimmunogenic to human body; small particle size (<100nm); BBB targeting; stable in blood; prolonged circulation time; ability to escape reticuloendothelial system (RES) etc. (Lockman et al., 2002).

Up to now, many researches have been carried out on polymeric and lipid nanoparticles to cross the blood brain barrier. Table 2.4 below gives a summary of various drugs loaded nanoparticles being delivered to the brain. Among them, polysorbate 80 or tween 80 coated polybutylcyanoacrylate (PBCA) nanoparticles are the most well studied system which has successfully delivered a number of therapeutic agents such as hexapeptide dalargin, doxorubicin, loperamide and amitriptyline to the brain of rats or mice. Polysorbate coated nanoparticles not only deliver these drugs that normally can't cross BBB but also increase the plasma half-life of these drugs due to their favorable surface characteristics. Moreover, CNS availability of these drugs also increases through sustained release (Kreuter, 2001; Alyautdin et al., 1997, Schroder and Sabel, 1996; Gulyaev et al., 1999, Chen et al., 2004). Despite the success of tween 80 coated PBCA nanoparticles being transported to the brain, there is always dispute on whether the polysorbate coated PBCA nanoparticles have toxic effect on BBB. Oliver et al. suggested

that the breakdown of PBCA nanoparticles by ubiquitous esterases would cause toxic effect on BBB based on a co-culture system. They also observed a mortality of mice (3 to 4 out of 10 mice) caused by PBCA nanoparticles. Thus they proposed the possibility of nonspecifically opening of tight junctions between endothelial cells in brain microvasculature by PBCA nanoparticles. However, Gelperina et al. reported no mortality or weight loss of rats after injection of doxorubicin loaded PBCA nanoparticles with polysorbate 80 as surface coating and the authors suggested the toxicity of doxorubicin loaded nanoparticles were similar or even lower than that of pure doxorubicin. By investigating the mechanisms of how PBCA nanoparticles deliver drugs across BBB, Kreuter et al. also suggested there was no toxicity effect of nanoparticles on BBB (Oliver, et al., 1999; Gelperina et al., 2002; Kreuter et al., 2003).

Table 2.4 Summary of drug loaded biodegradable nanoparticles across BBB

NP Matrix	Drug	Surfactant	Size(nm)	Results
PBCA	dalargin	tween 80	260	increased latency by 50% in analgesia study (Schroder et at., 1996)
PBCA	loperamide	tween 80	290	increased latency by 60% in analgesia Study (Alyautdin et al., 1997)
PBCA	doxorubicin	tween 80	270	~6mg drug/g brain at 2-5 hours, vs. 0 without carriers (Gulyaev et al., 1999)
stearic acid	doxorubicin	Epikuron 200	90	~1/4 of plasma with drug after 4 hour vs.0 in brain without carrier(Fundaro, et al., 2000)
Emulsifying Wax & Brij 78	--	PEG-thiamine	67	65% injected does (ID) in circulation, 0.5% ID in brain after 6 hours via i.v. injection, facilitated binding to BBB thiamine transporters, no significant enhance in brain uptake (Lockman, et al., 2003)

PLA	FITC-dextran	tween80	~200	observed fluorescence in rat brain after i.v. injection of fluorescent dextran loaded NPs (Sun, et al,2004)
Emulsifying Wax & Brij 78	paclitaxel	tween 60	~60	significant increase in brain uptake in *in vitro* cell line experiment & in situ brain perfusion. (Koziara et al., 2004)

Apart from polysorbate surface coatings such as polysorbate 20, 40, 60, 80, 85, many other coatings have also been tried by researchers such as PEG, poloxamer 407, poloxamer 338, polaxamer 188 (Borchardt, 1994). Although they showed prolonged circulation and increased uptake in *in vitro* BBB models, they failed to have the same effect in *in vivo* systems (Chen, et al., 2004).

To date, the exact mechanism of nanoparticles across BBB hasn't yet been known. However, it is highly possible that nanoparticles may be endocytosed or transcytosed through endothelial cells. Polysorbate 80 is believed to be an anchor of Apo E protein which can help nanoparticles mimic lipoproteins and interact with LDL receptors in endothelial cells leading to their uptake by brain endothelial cells (Kreuter, 2004).

2.4 Magnetic Resonance Imaging (MRI) and MRI Contrast Agent

2.4.1 Basic Principles of MRI

Magnetic resonance imaging (MRI) is to apply the phenomenon of nuclear magnetic resonance (NMR) to the field of imaging. The first MRI test was made in 1977, four years after the first NMR image was obtained by Paul Lauterbur. MRI is a technique that relies on the inherent magnetic properties of molecules in the body. Protons from water molecules will shift their orientations and form a net magnetization vector when a strong

static magnetic field B0 is applied to the body. A radiofrequency (RF) pulse, which ranges from approximately 10 to 200MHz, is used to knock some of the protons out of alignment. Weak radio signals will be released by protons as they shift back to their aligned position after the radio transmitter is turned off. Different tissues will have different strength and duration of these signals, thus the quantity of water in each tissue can be determined. Then the computer will use different slices to generate a 3D image. Basically, an MRI system consists of a magnet assembly, RF coils, a computer and a display device. MRI is a safe and powerful imaging tool with high resolution and can detect regions that can't be detected by other imaging tools such as CT, X-ray. MRI can also be used to detect tumors since it can tell the differences between normal and diseased tissues.

2.4.2 Important Parameters of MRI

It is important to understand the three principal parameters of MRI: proton density (PD), T1 relaxation time and T2 relaxation time. They are fundamentally different from and independent of each other. Through changing the type of RF pulse sequence and times, images weighted by each of the three parameters can be obtained (Bushong, 2003).

(1) *Proton Density*. Proton density, also referred to as hydrogen density, is the concentration of mobile hydrogen within tissues. The amplitude of the initial MR signal is related to the proton density in the tissue being imaged. If there is more hydrogen, stronger MR signal may be expected. The MR signal also depends on how hydrogen is bound within a molecule. The received MR signal only originates from loosely bound

mobile hydrogen and tightly bound hydrogen only has a weak signal.

(2) *T1 relaxation time*. T1 relaxation time, which is also called longitudinal time, or spin-lattice relaxation time, is the time needed to align protons in a static magnetic field. T1 constant indicates the speed of the spinning nuclei to emit their absorbed RF into the surrounding tissues. T1 is a tissue specific time constant and the value ranges from milliseconds to several seconds. For example, the average T1 for soft tissue is 600ms. T1 is longer in solids than in liquids. Generally, for T1 weighted images, tissue with short T1 appears bright while tissue with long T1 appears dark. The reciprocal of T1, 1/T1 is called longitudinal relaxation rate, which can also be represented by the symbol R1 in the unit of ms^{-1}. The slop of R1 over contrast agent concentration is called longitudinal relaxivity.

(3) *T2 relaxation time*. T2 relaxation time is transverse time, or spin-spin relaxation time, which is the time needed for protons to lose their coherent energy in an NMR measurement. T2 represents a loss of transverse magnetization. T1 and T2 are independent; however, T2 relaxation time never exceeds T1 in a given tissue. Generally speaking, for T2 weighted images, tissue with short T2 appears dark while tissue with long T2 appears bright. Similarly, 1/T2 equals the transverse relaxation rate R2 and the slop of R2 over contrast agent concentration is called transverse relaxivity.

Besides the three parameters above, T2* is often used to combine the real T2 of tissues and the magnetic field inhomogeneities.

2.4.3 Introduction to MRI Contrast Agent

The addition of contrast agent by injection before or during MRI procedure can improve the sensitivity and specificity of the images obtained. Briefly, there are two kinds of contrast agent: positive contrast agents and negative contrast agents (MRI technology website).

(1) *Positive contrast agents (appearing bright on MRI).* They are typically small molecular weight compounds containing gadolinium, manganese or iron as active elements which have unpaired electron in outer shells. They act predominantly on T1 relaxation, which results in signal enhancement. The most common and commercial available products of positive contrast include Gadopentate dimeglumine (Gd-DTPA), Gadoterate meglumine (Gd-DOTA), Gadodiamide (Gd-DTPA-BMA) etc. Gd-DTPA received approval from FDA in 1988 (Runge, 2000) and has been widely used in neuron and whole body imaging. Fig 2.6 below shows the chemical structure of Gd-DTPA from Sigma with a molecular weight of 547.57.

(2) *Negative contrast agent (appearing dark on MRI).* They are small particulate aggregates often termed superparamagnetic iron oxide (SPIO). They act predominantly on T2 relaxation, which results in signal reduction. However, particles smaller than 300nm also produce substantial T1 relaxation. Fig 2.3 below also gives the chemical structure of a widely used negative contrast agent Fe_3O_4-dextran.

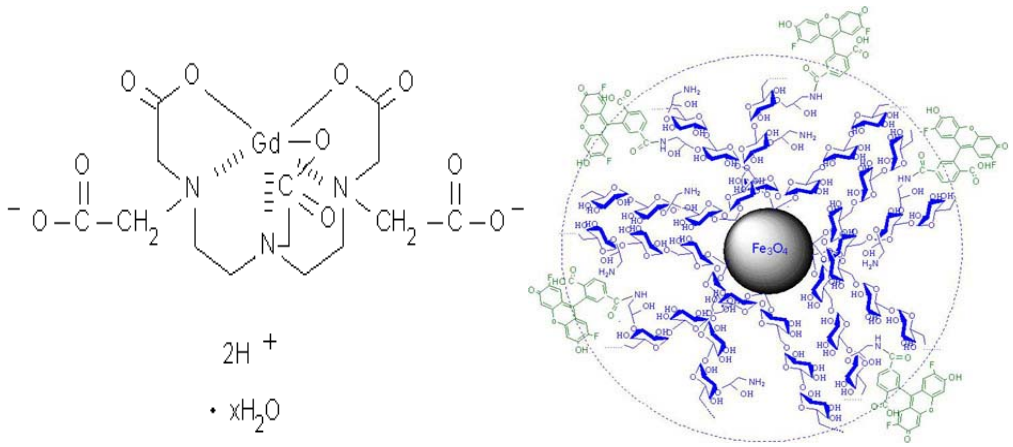

Fig 2.3 Chemical structures of Gd-DTPA and Fe_3O_4-dextran

In addition, macromolecular paramagnetic contrast agents, ultrasmall superparamagentic iron oxide (USPIO) particles are also studied world wide in multicenter clinical trials. Runge et al. had an excellent review on contrast agent used in brain disease (Runge et al., 1997). Moreover, a wide variety of vector and carrier molecules, including antibodies, peptides, proteins, polysaccharides, liposomes and nanoparticles have been developed to deliver magnetic labels to specific sites (Schmiedl et al.,1989; Wang et al., 1990; Runge, 2001; Morel et al., 1998; Faranesh et al., 2004). Recently, some groups begin to do research on gadolinium loaded nanoparticles not only for imaging but also for neutron capture therapy since gadolinium itself has effect on tumor cells (Shikata et al., 2002; Oyewumi et al., 2004; Watanabe, et al., 2002).

Chapter 3

Materials and Methods

3.1 Materials

Paclitaxel was purchased from Dabur India Limited, India and Hande Biotechnology Inc. (Kunming, China). Poly ($_{D,L}$-lactide-co-glycolide) (PLGA, 50:50, MW 40000-75000), Cormarin-6, polyvinyl alcohol (PVA, MW 30000-70000), Gadolinium Diethylenetriaminepenta-acetic Acid (Gd-DTPA, MW 547.57), MTT([3-(4,5-dimethylthiazol-2-yl)-2,5-diphenyltetrazolium bromide]), Trypsin-EDTA and gelatin (type B, 225 bloom), Hank's Balanced Salt Solution (HBSS), Penicillin Streptomycin, Dulbecco's Modification of Eagle's Medium (DMEM), and Phosphate Buffer Solution (PBS) were purchased from Sigma-Aldrich Chemical Co., Singapore. Vitamin E succinate with polyethylene glycol 1000 (Vitamin E TPGS) was provided by Eastman Chemical Company (TN, USA). DPPC (1,2-dipalmitoyl-sn-glycerol-3-phospatidylchlorine) was purchased from Avanti Polar Lipid, Inc. (Alabaster, A1, USA). Tween 80 was provided by ICN Biomedicals, Inc. (Ohio, USA). Commercial fluorescent polymer microsphere suspension or dyed polymer microsphere suspension (polymers include polystyrene (PS), polystyrene divinylbenzene (PSDVB), or other styrene copolymers) was bought from Duke Scientific Corporation (CA, USA). Dichloromethane (DCM, analytical grade) and acetone were purchased from Mallinckrodt Company (MO, USA). Acetonitrile for HPLC/ Spectro use (FW=41.05) was purchased from Tedia Company, Inc (Fairfield, OH, USA). Madin-Darby canine kidney (MDCK) epithelial cell

line was purchased from American Type Culture Collection (Manassas, VA, USA) and passages 58-70 were used. Rat glioma cell line C6 was also purchased from the same company. Fetal calf serum was purchased from Hyclone Company (UT, USA). Mounting medium was provided by Dako Corporation (CA, USA). PI (propidium iodide) was purchased from Molecular Probes, Singapore. Triton® X-100 was purchased from BDH limited (Poole, England). Male Sprague Dawley rats, 180-220 gm each and 6-8 week old, were supplied by the Laboratory Animals Centre of Singapore and maintained at the Animal Holding Unit of NUS. Deionized water produced by Millipore (Millipore Corporation, Bedford, OH, USA) was used throughout the whole experiment. MPEG-PLA was provided by Mr. Dong Yuancai and Mr. Zhang Zhiping.

3.2 Methods

3.2.1 Preparation of Nanoparticles

3.2.1.1 Preparation of Paclitaxel/fluorescence Loaded Nanoparticles- Single Emulsion

The PLGA nanoparticles were prepared by the oil-in-water solvent evaporation/ extraction technique. Altogether three samples were prepared: PVA emulsified nanoparticles, PVA &DPPC emulsified nanoparticles, vitamin E TPGS emulsified nanoparticles. Briefly, Paclitaxel 5.5mg and PLGA 110 mg were dissolved in 8 mL dichloromethane (DCM). DPPC 30mg was also dissolved in DCM. The resulted organic solution was then votexted for half a minute. The dissolved oil phase mixture was then poured slowly into the aqueous phase containing different emulsifiers (either 0.6 g PVA

or 36 mg Vitamin E TPGS dissolved in 120mL de-ionized water). The resulting emulsion was sonicated with an energy output of 25 W in a continuous mode for 90s.The formed oil in water emulsion was then stirred overnight at room temperature with the magnetic stirrer to evaporate the organic solvent (DCM). The produced nanoparticles were collected by centrifugation (11500 rpm, 12 min, 20°C) and washed with de-ionized water three times to remove excessive emulsifiers. The frozen product was then freeze-dried at -51 °C to get into fine powders of nanoparticles and kept in a vacuum desiccator for future use.

The fluorescent nanoparticles were prepared using the same method above while 0.55mg cormarin-6 was used as fluorescent marker instead of paclitaxel. Since coumarin-6 was light sensitive, the whole process should be done in dark.

3.2.1.2 Preparation of Gd-DTPA Loaded Nanoparticles- Nanoprecipitation

Nanoprecipitation can be used to encapsulate both hydrophilic and hydrophobic substances. Briefly, 75mg polymer (PLGA or MPEG-PLA) was dissolved in 5mL acetone. 0.3mL Gd-DTPA (15% w/v) was suspended in the polymer solution and sonicated for about 20 seconds. The resulted suspension was added drop by drop using a syringe to 25mL water with 100mg F-68. The formed emulsion was then stirred overnight at room temperature with the magnetic stirrer to evaporate the organic solvent. The nanoparticles were collected by centrifugation (12,000rpm, 18°C, 60 min) and washed with de-ionized water twice to remove excessive Gd-DTPA and F-68. Finally, the frozen product was then freeze-dried at -51°C to get into fine powders of nanoparticles..

3.2.1.3 Preparation of Gd-DTPA Loaded Nanoparticles- Double Emulsion

Double emulsion is often used to encapsulate hydrophilic substances. Briefly, 75mg polymer was dissolved in 5mL DCM, 0.3mL Gd-DTPA (15% w/v) was then added to the oil phase. The resulting solution was sonicated for 40s, and then added to 30mL water with certain emulsifier. The water-in-oil-in-water suspension was sonicated for 90 seconds. The formed emulsion was then stirred overnight at room temperature with the magnetic stirrer to evaporate the organic solvent (DCM). The produced nanoparticles were collected by centrifugation (11500 rpm, 15 min, 12 ^{0}C) and washed with de-ionized water three times to remove excessive emulsifiers. The frozen product was then freeze-dried at -51 ^{0}C to get into fine powders of nanoparticles.

3.2.2 Characterization of Nanoparticles

3.2.2.1 Size and Size Distribution

Particle size and size distribution were measured by laser light scattering system with particle size analyzer (90 Plus, Brookhaven Instruments, Huntsville, NY, USA) at 25ºC with a scattering angle of 90º. For the measurement, ~0.lmL nanoparticle suspension before freeze-drying was dispersed in 1 mL de-ionized water in a plastic cuvette, which was sonicated for 1minute. The cuvette was wiped clean and placed inside the machine for measurement. The laser will shine through the cuvette and take the reading. Information gathered would determine the mean diameter and size distribution which is also known as polydispersity.

3.2.2.2 Particle Morphology

(a) Scanning Electron Microscopy (SEM)/Field Emission Scanning Electron Microscopy (FESEM)

The particle size, shape and surface morphology of the nanoparticles prepared earlier could be characterized by SEM/FESEM (Jeol, JSM-5600 LV**,** Irfan View software).A small spatula of the sample was placed on to a black double-sided sticky tape, taped to the SEM/FESEM stud. They were then coated with platinum, performed in an Auto Fine Coater for 40s in a vacuum at a current intensity of 40mA (JFC-1300, JEOL, USA) before SEM/FESEM analysis. After SEM/FESEM captured the images, the sizes of the particles could be measured using Irfan view software.

(b) Atomic Force Microscopy (AFM)

The surface morphology and particle size could also be characterized by AFM (Multimode^{TM} Scanning Probe Microscope, Digital Instruments, USA). The nanoparticles were attached to double side sticky tape before atomic force microscopy (AFM) was conducted. Thereafter, AFM images were obtained by Nanoscope Ⅲa (Digital Instrument, Santa Barbara, CA, USA) in tapping mode. The cantilever oscillated at its proper frequency (~300 KHz) and the driven amplitude was ~130 mV.

3.2.2.3 Surface Charge

Surface Charge was measured using ZetaPlus^{TM}Zeta Potential Analyzer (Brookhaven Instrument Corp, Holtsville, NY). Briefly, ~0.1mL nanoparticles suspension before freezedrying was dispersed in 1 mL water, which was followed by sonication for 1min. Then the mixture was poured into a plastic cuvette. The zeta potential of products was

measured with palladium electrodes, which was cleaned with de-ioned water before inserting into the cuvette. The cuvette was then placed inside the analyzer for surface charge analysis and the mean of the five readings was taken.

3.2.3 Encapsulation Efficiency and Drug Entrapment

3.2.3.1 Encapsulation Efficiency and Drug Entrapment of Paclitaxel loaded Nanoparticles

This experiment was performed in triplicates using high performance liquid chromatography (HPLC) (Agilent LC1100) to determine the concentration of paclitaxel. A reverse phase Inertsil ® ODS-3 column (150x 4.6 mm i.d., pore size 5µm, GL Science, Tolyo, Japan) was used. 3 mg nanoparticles were dissolved in 1 mL DCM to extract paclitaxel from the nanoparticles. DCM was allowed to evaporate overnight. 3 mL acetonitrile/ water (50:50, v/v) was added and the solution was votexed for 1 min. After that, the sample was transferred to HPLC vials. The formulations that were used to calculate EE and drug entrapment were:

$$\text{Encapsulation Efficiency (EE) (\%)} = a/b \times 100;$$

$$\text{Drug Entrapment (\%)} = a/c \times 100$$

where a is the amount of drug in nanospheres; b is the amount of drug used for fabrication; c is the amount of nanospheres. To avoid the influence of inefficient extraction, the extraction efficiency was also measured in this experiment. Briefly, certain amount of pure paclitaxel similar to the amount loaded in the corresponding amount of nanospheres and 3 mg placebo nanoparticles were dissolved in 1mL DCM. 3 mL of

acetonitrile/water were added and the same extraction procedure was done as described above. The resulting factor was 100%, which means no loss in the extraction procedure.

3.2.3.2 Encapsulation Efficiency and Drug Entrapment of Gd-DTPA loaded Nanoparticles

This experiment was studied by inductively coupled plasma-optical emission spectrometry (ICP-OES) and was done in triplicates. Briefly, 25 mg nanoparticles were dissolved in 3mL DCM and votexed for 1min. DCM was evaporated overnight. 3mL of Millipore water was added to extract Gd-DTPA. Then the samples were filtered by 0.22μm filter. The concentration of Gd was determined by ICP-OES.

3.2.4 *In Vitro* Release

3.2.4.1 *In Vitro* Release of Paclitaxel Loaded Nanoparticles

The release of paclitaxel from the nanoparticles was measured using high performance liquid chromatography (HPLC). 5 mg paclitaxel loaded nanoparticles were weighed into individual centrifuge tubes and suspended in 10 mL of fresh PBS (pH=7.4). The tubes were placed in a 37^{o}C orbital shaker water bath and shaken horizontally at 120 min^{-1}. The experiment was done in duplicates. The tubes were taken out at particular time intervals and centrifuged at 12000, 18^{o}C, 18 minutes. The supernatant was removed and taken for *in vitro* release analysis. The precipitated nanoparticles were re-suspended in 10 mL PBS, sonicated, vortexed and placed back into the water bath shaker. Paclitaxel in the supernatant was extracted in 1 mL DCM in a separation funnel. The funnel was shaken consistently and 2 layers would form. The top layer contained water while the bottom

layer contained DCM and the extracted paclitaxel. DCM was collected and allowed to evaporate overnight. 3 mL of acetonitrile/ water (50:50,v/v) was added after evaporation and conditions for HPLC analysis were the same as mentioned above. Similarly, the extraction recovery coefficient was also measured using the same method mentioned above except that paclitaxel was in aqueous phase instead of dissolving in DCM directly. The extraction factor was around 80% and the data obtained for *in vitro* analysis was corrected accordingly.

3.2.4.2 *In Vitro* Release of Gd-DTPA Loaded Nanoparticles

This experiment was done in a similar way as the *in vitro* release of paclitaxel loaded nanoparticles. Briefly, 30mg nanoparticles were suspended in 5mL PBS. At pre-determined time the samples were centrifuged and the supernatant was taken out for analysis. Since the Gd-DTPA released much faster than paclitaxel, the release file was obtained within 48 hours. The resulted released gadolinium in PBS was measured directly by ICP-OES. The study was also carried out in duplicates.

3.2.5 Cell Line Experiments

3.2.5.1 Cell Culture

The glioma cells C6 and MDCK were grown in 25 mL flasks, and maintained in a humidified 5% CO_2/95% air incubator at 37^0C in medium (DMEM+10% FBS+5% penicillin G). The medium was changed every two days until the cells reached 80-90% confluence. After that, the cells were harvested with trypsin.

3.2.5.2 Trypsinization Procedures of the Cells

The aim of trypsinization was to detach the cells from the bottle wall and collect the cells to transfer to the 96-well plate and estimate the density of the cells. Cells seeded in culture flasks were observed every 2 days, culture medium were changed every 2 days till cells reached ~85% confluence. The PBS and medium were warmed in the 37^{o}C water bath. Trypsin should not be warmed up as heat could inactivate the enzyme. The medium was removed from the culture flask and the flask wall was washed with 5 mL PBS twice. 1 mL trypsin was added to the bottle and shaken gently before removing them. Then 1 mL trypsin was added again and incubated for about several minutes at 37^{o}C, 5% CO_2 until detached cells were seen floating in trypsin. 5.5 mL medium was introduced to the bottle and pipette was used to make the cells even distributed. It was then transferred to a small centrifuge tube and centrifuged 800rpm, 6 minutes. The supernatant was discarded and the pellets were evenly suspended in 4.5 mL medium. 100µl cell suspension was taken out to estimate the density under the microscope. The cell density is: the sum of the cells in the four squares (4x4)/4*10^4cells/mL.

3.2.5.3 Cell Viability Study/Cytotoxicity Study

Cell viability/cytotoxicity study can be done with the MTT assay. The aim of this study was to measure quantitatively how much cells would be killed with the drug-loaded nanoparticles. Cell viability of nanoparticles with no drug and pure drug should also be tested as control. First, seed cells on 96 well plate (seeding density=1.3x10^4 cells/well) and wait for cells to grow until 80% confluence. Then, HBSS (Hank's Balanced Salt Solution) stock with H_2O and PBS [since both HBSS and PBS are concentrated (10x),

need to dilute using 1 part of HBSS to 9 part of PBS (1 part of PBS to 9 part of Millipore water)] was prepared. The cells with prepared HBSS medium were equilibrated and incubated for 1 hour. Then the HBSS was removed and nanoparticle suspensions, pure drug solution in DMEM were added. After incubating for a pre-determined time, the suspension was removed and washed with PBS twice. MTT solution was prepared by diluting concentrated MTT with PBS to 5mg/mL. MTT is light sensitive, henceforth must protect the stock bottle from light. After that, 90μl DMEM medium and 10μl MTT were added into the plate. The cells were incubated for 4 hours. After which, purple ppt was seen. Remove the media without removing the bluish ppt. Then dissolve the ppt with DMSO solution of 200μl each well. After that, the plate was placed inside a micro-plate reader and read the absorbance using 560 nm filter.

3.2.5.4 Cell Uptake Study

The aim of the cell uptake study was to find out how much fluorescence loaded nanoparticles would be taken by the cells. The previous step was similar to the procedure taken by the viability study until the cells had been treated with HBSS and incubated for 1hour. In the mean time, nanoparticles with different sizes and different surface coatings were prepared and suspended in Millipore water. The particle suspensions were sonicated so that the particles would not settle at the bottom. The experiment on the 96 well plate was planned to include negative controls (cells only with no particles added), positive controls and samples. HBSS was then removed from the wells and incubated with 100 μl of the particle suspensions added to designated wells for 4 hours at 37^{o}C. After incubation, particle suspensions and HBSS were removed only from the sample wells and

from the cell-only wells respectively. The cells in the sample wells and negative control wells were washed 3 times with PBS, mainly to remove excess nanoparticles that were not taken up by the cells. To the positive controls which should equivalent to 100% initial particle suspension seeded, 50 µl of triton/0.2M NaOH were added. 50µl PBS and 50 µl 0.5% triton/0.2 M NaOH were added to the samples and cell-only wells. The plate was then scanned with a microplate reader (excitation wavelength 430 nm, emission wavelength 485 nm) to measure the amount of fluorescence in each well.

3.2.5.5 Fluorescence Microscopy and Confocal Study

The aim of fluorescence microscopy and confocal study was to give direct evidence that nanoparticles had really come into the cells. The MDCK cells were seeded in the 24-well assay white plate with coverglass seated in each well. The cells were incubated at 37^{o}C, 5% $CO_{2.}$ The medium was changed every two days until the cells reached 70% confluence for all wells. When the required confluence was reached, the medium was removed from the plate and replaced with 500µl fresh HBSS. Cells were equilibrated by incubating at 37^{o}C, 5% CO_2 for 1 hour. In the mean while, certain concentration nanoparticles were prepared and suspended in HBSS. The particle suspensions were sonicated so as to ensure even distribution and the particles did not settle at the bottom. HBSS was then removed from the plates and incubated with the particle suspension for 4 hours. After incubation, the particle suspension and HBSS were removed from each well. 500µl ethanol was added to fix the cells. Then the plate was placed in the incubator for 20 minutes. After that, the ethanol was removed and the cells were washed with PBS for 3 times. 200µl PBS was re-added and 20~30µl propidium iodide (PI) was added to stain the nucleus. The plate was placed in the incubator for another 40 minutes. After

incubation, PI was removed and the wells were washed with PBS for three times. 2~3 drops of mounting medium were added to the cells. At last, cells could be examined under the fluorescence microscope or confocal microscope (Zeiss LSM 410, Germany) equipped with imaging software, Fluoview FV300.

3.2.6 Animal Study

Healthy rats were divided into three groups in *in vivo* experiments. One group was treated as control and would inject only 0.9%(w/v) NaCl saline. In the other two groups, the rats were intravenously injected with fluorescent nanoparticle solutions coated or uncoated with tween 80. After injection, the rats would be placed in the cage for 1.5 hours and the blood vessels of the rats would be rinsed before sacrificing them to bring out the brain. The bought-out rats' brains were put into 4% paraformaldehyde solution to be fixed. After that, tissue freezer was used to freeze the brain tissues. Cyrostat (Leica, CM3050) was used to cut the tissue into slices of 10 μm thick. The resulted slices would be observed under fluorescence microscopy.

3.2.7 MRI Characterization

The MRI characterization of Gd-DTPA encapsulated nanoparticles and the calibration curve of pure Gd-DTPA were measured on a 1.5T scanner with a head coil using a clinical MRI machine, National University Hospital (SIMENS). Briefly, Gd-DTPA encapsulated nanoparticle samples of a certain concentration and standard Gd-DTPA solution ranging in concentrations from 0 to 2mM were prepared both in water and in gelatin. Then they had a MR scanning with the following parameters: slide thickness =

5mm, TR ranging from 25ms to 6400ms, TE=12ms, FOV=180 and FOV phase= 100%. The surrounding temperature remained at 22^{o}C in all experiments to reduce the effect of temperature dependence on relaxation rate. Signal intensities were measured from a region of interest in the center of the samples and would be transferred through a self-developed program by NUH staff to get the corresponding T1, T2 values. Then their characteristics were analyzed.

Chapter 4

In Vitro Study of Paclitaxel Loaded PLGA Nanoparticles to Treat Brain Cancer Cells

4.1 Novel Formulation of PLGA Nanoparticles with Natural Emulsifiers

Emulsifiers, also known as surfactants, play an important part in the process of fabricating nanoparticles. The emulsifier serves to 'link' up the oil phase and the aqueous phase during the formulation process (Mu and Feng, 2002). This linkage between the two immiscible phases stabilizes the emulsion and allows the formation of nanoparticles. This emulsion is possible since the emulsifier, which contains both hydrophilic and hydrophobic parts, helps to stabilize the dispersed or dissolved polymer and drug molecules by keeping them 'apart' and hence prevents the aggregation of these particles. Moreover, the remaining emulsifiers on the nanoparticle surface serves as surfactant may further affect nanoparticles' characteristics.

Compared with traditional chemical emulsifier PVA, novel natural emulsifiers vitamin E TPGS and DPPC have more advantages. Both of them are natural surfactants which are biocompatible and do no harm to human body while residual PVA on the nanoparticles' surface may cause some side effects. Moreover, both vitamin E TPGS and DPPC have amphiphilic structures, which make them good candidates to act as emulsifiers and surface coatings. Fig 4.1 below shows the chemical structures of PVA, vitamin E TPGS and DPPC.

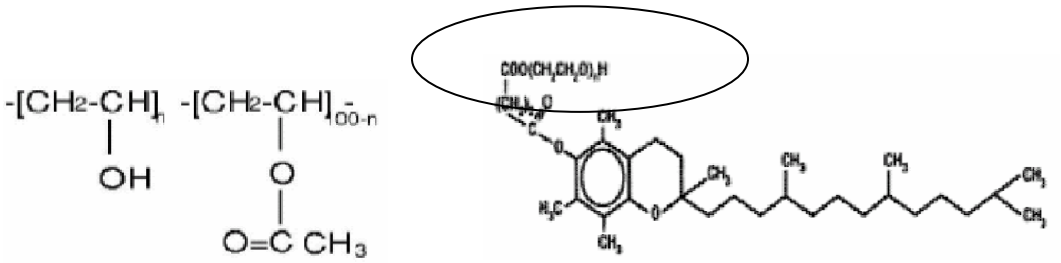

PVA vitamin E TPGS

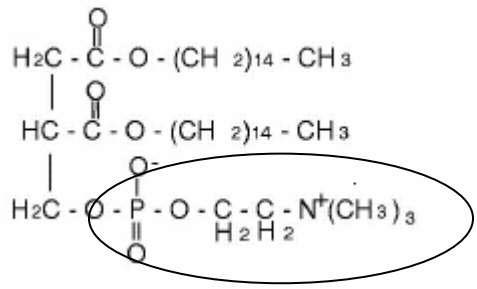

DPPC

Fig 4.1 Chemical structure of PVA, vitamin E TPGS and DPPC

Vitamin E TPGS is a water-soluble derivative of natural vitamin E, formed by esterification of vitamin E succinate with polyethylene glycol 1000. It has dual nature with part of the molecule showing hydrophobicity while another part showing hydrophilicity. From Fig 4.1 above, it can be seen that the polyethylene glycol portion (indicated in the circle) acts as the hydrophilic polar head and the tocopherol succinate portion (on the other end) behaves as the lipophilic tail. Vitamin E TPGS can not only dissolve well in water but also in oil. This special structure property suggests its potential application as emulsifier. Unlike PVA, vitamin E TPGS can form solution with water at a concentration of up to 20% (w/w), beyond which high viscosity liquid crystalline phases begin to form. However, the critical micelle concentration (CMC) of TPGS is only about 0.02 wt% in water beyond which TPGS will begin to form micelles and continue to form low viscosity solutions till reach the concentration of 20%. If the concentration of TPGS

is too low in water, it won't act as an emulsifier. However, if it is too high, TPGS tends to self-assemble to form micelles and change the state in the aqueous dispersing phase. Mu and Feng found that the optimal concentration for TPGS as emulsifier was 0.02%-0.03%, which resulted in best nanoparticle yield and size (Mu and Feng, 2003).

In the same way, natural phospholipid DPPC also has amphiphilic structure. From the chemical structure of DPPC in Fig 4.1, it is clear that DPPC has a hydrophilic head (the part in the circle) and a hydrocarbon tail. In the following experiments, these two novel emulsifiers will be used to fabricate the paclitaxel/fluorescence loaded nanoparticles of biodegradable PLGA nanoparticles and their potential to cross the blood brain barrier and to treat brain tumor will also be investigated.

4.1 Size, Size Distribution and Surface Charge

Table 4.1 Size, polydispersity and zeta potential of 5% paclitaxel loaded PLGA nanoparticles with different emulsifiers

Matrix/Emulsifier	Particle Size (nm)	Polydispersity	Zeta Potential (mV)
PLGA /PVA	267.3	0.076	-13.80
PLGA/DPPC&PVA	245.2	0.066	-15.70
PLGA/vitamin E TPGS	284.8	0.048	-28.82

Table 4.1 above shows the particle size, size distribution and surface charge of 5% paclitaxel loaded PLGA nanoparticles (5.5mg paclitaxel plus 110mg PLGA during fabrication) with different emulsifiers. Solvent extraction /evaporation (single emulsion) method was used to fabricate these nanoparticles. Altogether three batches of particles were fabricated and would be used for further investigations including PVA emulsified nanoparticles, DPPC emulsified nanoparticles with PVA as co-emulsifier in water phase

and vitamine E TPGS emulsified nanoprticles. The particle size and polydispersity were determined by LLS (laser light scattering). Zeta potential was determined by zeta potential analyzer. From the table, it can be seen that nanoparticles with size less than 300nm and a negative surface charge were achieved.

4.2.1 Particle Size and Size Distribution

Prior to fabricating the DPPC emulsified nanoparticles with PVA as co-emulsifier, the effect of DPPC alone as emulsifier both in water phase and oil phase was also investigated. Although DPPC possesses amphiphilic structures, it doesn't dissolve very well in the water phase, which reduces the effectiveness of its emulsifying efficiency. The size of the particle with DPPC as emulsifier in water phase was around 1700nm. Usually, nanoparticles for drug delivery to the brain are of diameter less than 400nm (Chen et al., 2004). Therefore it was not favorable for the purpose of crossing BBB. Although DPPC can dissolve well in the oil phase, the particle size of DPPC as emulsifier in the oil phase was still as much as 1000nm, which was still too large for our investigation purpose. The large particle size may be caused by the relative small molecular weight of DPPC which is only 734. Finally, we used DPPC as emulsifier in the oil phase and PVA in the water phase as co-emulsifier. From Table 4.1, it is clear to see that nanoparticles fabricated by this way not only has favorable size but also has good surface characteristics.

From table 4.1, it can also be seen that DPPC & PVA emulsified nanoparticles have a smaller particle size than that of naked PVA emulsified nanoprticles. The results may be

due to the additive effect of co-surfactant (Kreuter, 1994). The combination of PVA and DPPC increases the emulsifying efficiency, thus makes smaller size of the nanoparticles. Moreover, the polymer matrix PLGA was also dissolved in the oil phase; DPPC served not only as emulsifier but also part of the matrix and would affect nanoparticles' surface characteristics.

Vitamin E TPGS emulsified nanoparticles have a larger particle size than other two formulations. This may be due to the differences in the chemical structure of TPGS and PVA. From Fig 4.1, it can be seen PVA has a long linear chain structure with a high molecular weight up to 30,000-70,000, which makes it an effective emulsifier in stabilizing the oil droplets to form small nanoparticles. However, the molecular weight of vitamin E TPGS is only 1,513, which is less than 1/20 of that of PVA, thus makes TPGS emulsified nanoparticles have larger particle size. However, considering the amount of TPGS used in the fabrication (36mg) compared with PVA (600mg), we can still think the emulsifying efficiency of vitamin E TPGS is higher than that of PVA.

The size distribution was measured by laser light scattering system. In this system, the size distribution was specified in the light scattering intensity and polydispersity was defined as the log normal distribution width of the particle diameter. From Table 4.1, it can be seen that for all the three formulations, a narrow size distribution of 0.048~0.076 was achieved, which means the size of the nanoparticles is very uniform. This point can also be further confirmed by the SEM pictures shown below.

4.2.2 Surface Charge Study

Zeta potential is an indicator of nanoparticles' surface charge, which also determines the stability of nanoparticles in dispersion. Moreover, zeta potential can affect the characteristics of tissues. Lockman et al discovered recently that cationic and high concentration anionic nanoparticles would disrupt the integrity and permeability of the blood brain barrier while neutral and low concentration anionic nanoparticles would not. Thus only neutral and low concentration anionic nanoparticles were suitable to be used as drug carrier to the brain. They also discovered that the brain uptake rates of low concentration anionic nanoparticles were superior to that of neutral and cationic formulations at the same concentration (Lockman et al., 2004).

The surface charge of nanoparticles was measured by the Brookhaven zeta potential analyzer in this project. From Table 4.1, it could be seen that all three batches of nanoparticles were negatively charged which were suitable for brain uptake in low concentrations. The negative surface charge could be attributed to the presence of ionized carboxyl groups on nanoparticles' surface (Sahoo et al., 2002). Stolnik et al. reported that the zeta potential of naked PLGA nanoparticles without any PVA in neutral buffers was about -45mV (Stolnik et al., 1995). This high negative charge was primarily due to the uncapped end carboxyl groups of the polymer at particle surface.

Our samples showed a much lower negative charge than naked PLGA. For PVA emulsified nanoparticles, the zeta potential was -13.80mV, DPPC&PVA emulsified nanoparticles was -15.70mV, vitamin E TPGS emulsified nanoparticles was –28.82mV. The reduction in negative charge on particle surface should be attributed to the shielding

effect of the remaining emulsifier on particle surface which serves as surface coating or surfactant. Coating nanoparticles with these amphiphilic materials shields the surface charge and moves the shear plane outwards from the particle surface (Sahoo et al., 2002). It was found that a fraction of PVA used as emulsifier would form a stable inter-connected network with the polymer at interface during nanoparticle fabrication and would not be removed via the washing process (Carrio et al., 1991; Boury et al., 1995). For DPPC, because of its relative low solubility in water and blending with polymer in the oil phase during fabrication, a considerable fraction of it will also be remained in the particle surface. Feng & Huang found a dominant DPPC remained in DPPC emulsified nanoparticle surface using XPS (X-ray Photon Spectroscopy) detection (Feng and Huang, 2001). For vitamin E TPGS emulsified PLGA nanoparticles, they had a higher negative zeta potential than the other two batches but still lower than that of naked PLGA nanoparticles. This may due to the good solubility of TPGS in water and the small amount used (only 36 mg compared with 600mg PVA) during fabrication so that they can be relatively easily washed away. However, the lower negative zeta potential of vitamin E TPGS emulsified nanoparticles than naked PLGA nanoparticles indicates the existence of remaining TPGS on particle surface.

4.3 Surface and Bulk Morphology

Besides size, size distribution and surface charge, surface and bulk morphology of nanoparticles is also very important because it determines the drug release kinetics from the nanoparticles. Scanning electron microscopy (SEM) and atomic force microscopy (AFM) in tapping mode were used to give both general and specific morphology of the

nanoparticles. SEM needs prior coating of platinum on the surface of nanoparticles and can demonstrate morphology of bulk nanoparticles. As the voltage of instruments decreases, SEM images of higher amplification can be achieved without damaging the samples. In contrary to SEM, AFM doesn't need sample coating and can provide much higher resolution than SEM, thus more detailed surface morphology can be achieved. AFM can also demonstrate 3-D morphology of the nanoparticles.

Fig 4.2 to Fig 4.4 demonstrates the SEM and AFM images of all three batches of nanoparticles. From SEM, it can be seen that all nanoparticles had fine spherical shapes and smooth surfaces. There were some club-shaped things among nanoparticles, which was the drug that hadn't been encapsulated but remained on the surface of nanoparticles. AFM reveals the fine structures of nanoparticle surface and clear 3-D morphological images of spherical nanoparticles. It can also be seen that there was no aggregation or adhesion among nanoparticles. Although the multi-particle AFM images showed smooth surface as seen below, some researchers have done single particle zoom in (Mu & Feng, 2003) and particle sectioning analysis (Feng & Huang, 2000), which substantiated the existence of complex topography of nanoparticles indicating micro-caves and pores on the surface instead of simple smooth morphology. Though the structure of the nanoparticles could be quite complex, the relative smooth surface could be shown as an evidence to support the assumption that the release of drug from nanospheres might be caused by both polymer erosion and drug diffusion.

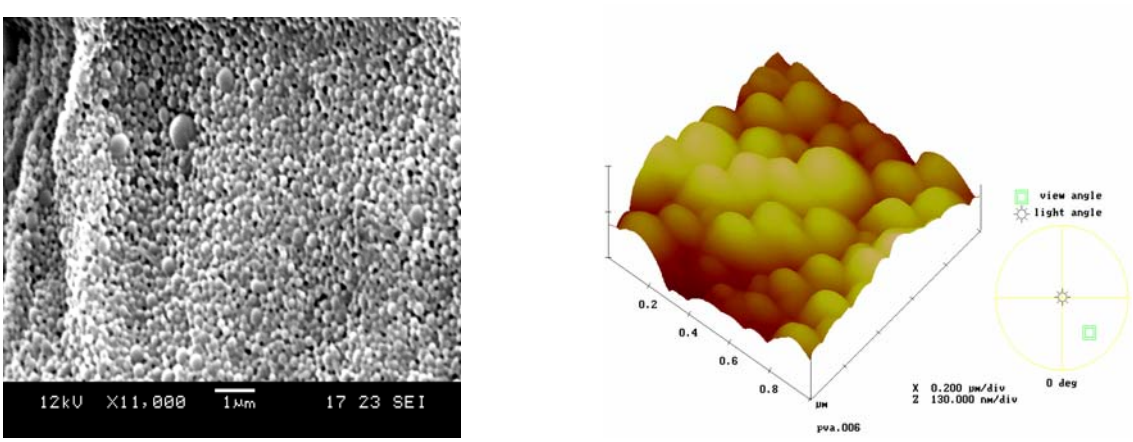

Fig 4.2 SEM and AFM images of PVA emulsified PLGA nanoparticles (5% drug loading)

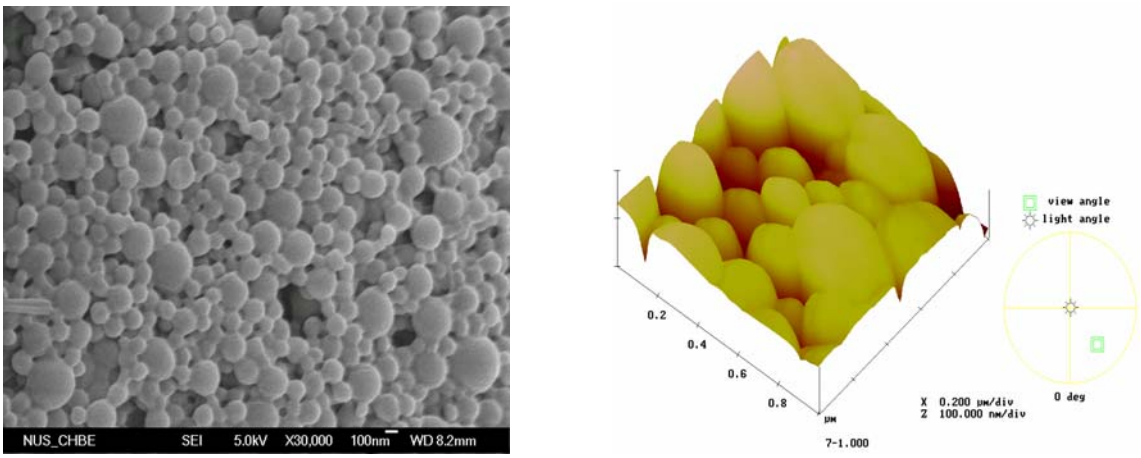

Fig 4.3 SEM and AFM images of PVA & DPPC co-emulsified PLGA nanoparticles (5% drug loading)

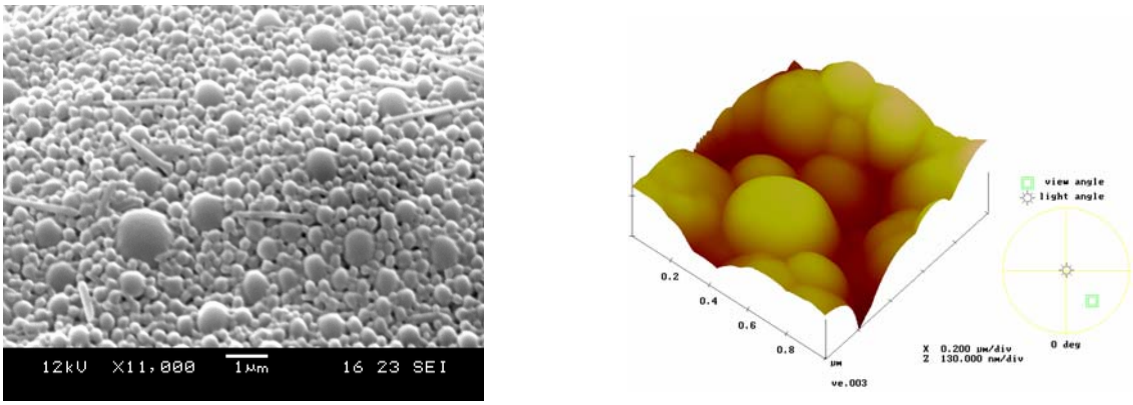

Fig 4.4 SEM and AFM images of vitamin E TPGS emulsified PLGA nanoparticles (5% drug loading)

4.4 Encapsulation Efficiency of Paclitaxel Loaded Nanoparticles

Encapsulation efficiency (EE) is the parameter to characterize the fraction of drugs incorporated into the nanoparticles compared with the original amount used in fabrication. EE is important in developing drug carriers since too low EE will prevent the mass production of drug loaded devices, especially for those expensive drugs such as paclitaxel. In this experiment, high performance liquid chromatography (HPLC) was used to measure the encapsulation efficiency of paclitaxel in PLGA nanoparticles and the experiment was done in triplicate.

From Fig 4.5 below, we can see all three batches of nanoparticles obtained favorable EE value. For PVA emulsified nanoparticles, the encapsulation efficiency was 58.42%, for DPPC&PVA emulsified nanoparticles, EE value was 45.71% and the encapsulation efficiency of vitamin E TPGS emulsified nanoparticles was 92.30%. The relative high encapsulation efficiency is attributed to the physiochemical characteristics of the drugs encapsulated. During the process of forming solid nanoparticles with extraction/evaporation method, not only organic solvent, but also the polymer and drug will partition or diffuse from internal organic phase to external aqueous phase, which results in the loss of drugs. Just as introduced previously, paclitaxel is very hydrophobic, thus most of it would stay in the polymer matrix even after repeated washing during fabrication. For hydrophilic drugs, the encapsulation efficiency won't be that high with the same extraction/evaporation method (Jain, 2000).

Besides the drug encapsulated, EE is also influenced by the polymer, the emulsifier, the method used to fabricate nanoparticles and the particle size. Generally, the larger the

particles, the higher the encapsulation efficiency and our result is correspondent with this principle. Vitamin E TPGS emulsified nanoparticles had the largest particle size and they also had the highest EE value. On the other hand, DPPC& PVA emulsified nanoparticles had the smallest particle size and they got the smallest encapsulation efficiency.

From Fig 4.5, we can also discover that the encapsulation efficiency of vitamin E TPGS emulsified nanoparticles is much higher than the other two batches. Although size may affect EE as discussed above, other factors such as the effect of emulsifiers must also be considered for this significant improvement. Vitamin E TPGS has large and bulky surface areas in its hydrophilic polar head portion and lipophilic alkyl tail, which might account for its effectiveness in preventing the partition or diffusion of hydrophobic paclitaxel from internal polymer matrix to external phase. The high encapsulation efficiency of vitamin E TPGS emulsified nanoparticles also improves the current solvent extraction/evaporation method (Mu and Feng, 2002).

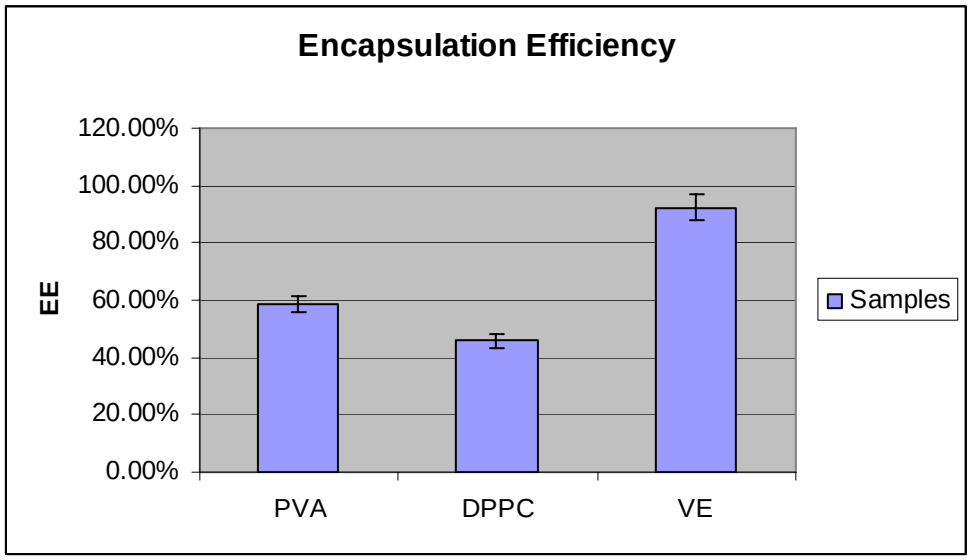

Fig 4.5 Encapsulation efficiency of PVA, DPPC and vitamin E TPGS emulsified PLGA nanoparticles(5% paclitaxel loading, n=3)

4.5 *In Vitro* Release Profile of Paclitaxel from Nanoparticles

One of the greatest advantages of applying nanoparticles as drug delivery device is the possibility of achieving "controlled release". By releasing drugs in a sustained manner, the drug concentration will be maintained within therapeutic index thus to reduce administration times and prolong the action of drug molecules. *In vitro* release kinetics is a very important parameter to measure the drug loaded devices.

Fig 4.6 shows the *in vitro* release profile of the three batches of nanoparticles after corrected with the extraction efficiency factor. The experiment was carried out in the phosphate buffer solution (PBS) of pH=7.4 at 37^{o}C in an orbital shaker as the simple simulation of human body environment. Release in about 1 month was measured. All batches of nanoparticles had a similar release profile with an initial burst in the first few days and later slow and sustained release in a nearly constant rate. For PVA emulsified nanoparticles, the initial burst was quite high with over 40% of drugs in the first three days; for DPPC&PVA emulsified nanoparticles, the initial burst was around 30% while vitamin E TPGS emulsified nanoparticles had the smallest initial burst of less than 20%. After 25 days, PVA emulsified nanoparticles released around 68% of all encapsulated drugs; DPPC& PVA emulsified nanoparticles released around 60% and vitamin E TPGS emulsified nanoparticle released the least percentage of around 40%. However, we can not say vitamin E TPGS emulsified nanoparticles released the least amount of drug since the encapsulation efficiency of it is much higher.

Recall the SEM pictures, not all drug molecules have been encapsulated into the nanospheres, there were some on the surface of the nanoparticles. The initial burst could

be caused by the diffusion release of paclitaxel distributed on or near the surface of nanospheres. Afterwards, the release rates slowed down because it needed time for paclitaxel to diffuse out from relative inner shell of nanoparticles. Swelling of the nanoparticles, which was caused by the absorption of the PBS solution, could also have occurred, leading to the release of drugs via dissolution. Since the degradation of polymers is very slow, the main mechanisms for drug release should be diffusion and matrix swelling.

The differences in initial burst and releasing rate of the three batches of nanoparticles may be caused by different properties of the emulsifiers. The addition of DPPC in fabrication formed a layer of coating on nanoparticles' surface, thus reduced the micro-caves and micro-pores on nanoparticle surface. Therefore, both the initial burst and release rate decreased for DPPC&PVA emulsified nanoparticles compared with naked PVA emulsified nanoparticles. Although smaller particles usually result in faster releasing rate, the DPPC&PVA emulsified nanoparticles with smaller particle size still had slower rate than PVA emulsified nanoparticles because the effects of emulsifier dominated over the releasing procedure. For vitamin E TPGS emulsified nanoparticles, firstly, their relative large particle size resulted in slower release rate; secondly, the ability for TPGS to dissolve well in both water and oil phase together with their bulky chains helped PLGA and paclitaxel have better interaction in fabrication thus further reduced the releasing rate. Although neutral PBS can act as a simple simulation of human body, it could not replace the real *in vivo* situation. Different pH values, ions and various proteins in blood can affect the release profile a lot (Verma et al., 2005).

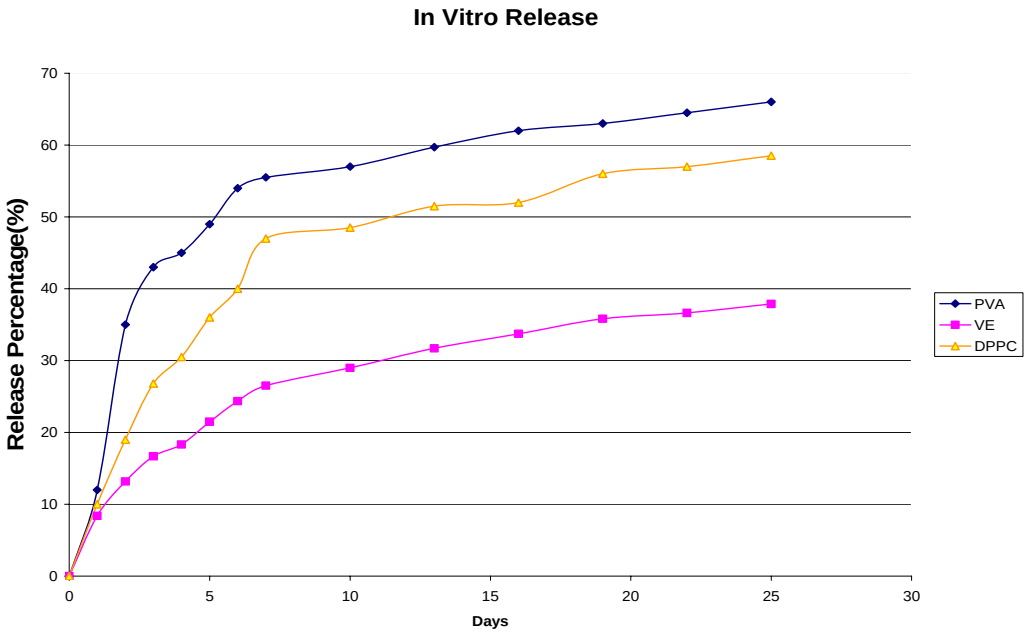

Fig 4.6 *In vitro* release profile of PVA, DPPC, vitamin E TPGS emulsified nanoparticles (5% paclitaxel loading)

4.6 Cell Culture of Rat Brain Tumor Cell Line C6

C6 is a kind of rat glial tumor cell line, which was used as a model cell line to study the cell viability in this project. Fig 4.7 below is the image of C6 cell line after 3 days' culture. This picture was also taken with the Olympus 1X700 optical microscope in chemotherapeutic engineering lab, NUS.

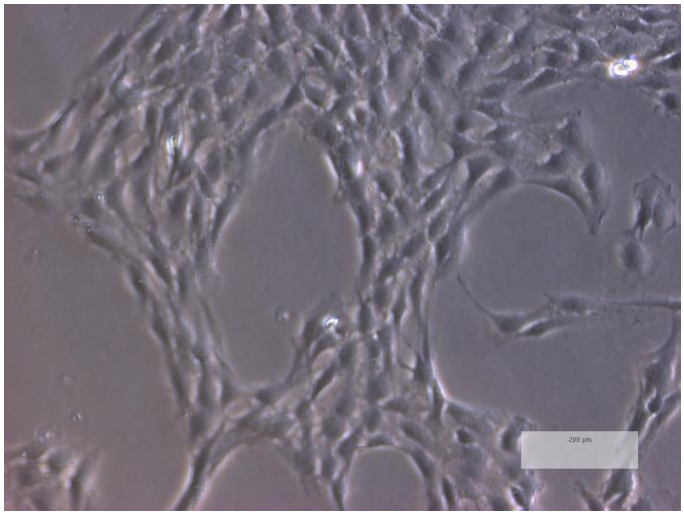

Fig 4.7 Morphology of rat brain glioma cell line C6 reaching ~50% confluence after ~ 3 days' culture

4.7 Cell Viability Study

To evaluate the potential of paclitaxel loaded nanoparticles to treat brain cancer, cell viability study was carried out using MTT assay with rat brain cancer cell line C6 as the model cell line. MTT assay is a laboratory test for measuring cellular proliferation (cell growth). MTT is added to a cell culture and is modified into a dye by enzymes associated metabolic activity in a live cell. The cell viability of commercial paclitaxel product Taxol® was also tested to do a comparison with the paclitaxel loaded nanoparticles.

Fig 4.8 and Fig 4.9 show the concentration effect and time effect in cell viability study of paclitaxel loaded nanoparticles and Taxol®. The initial drug loading was 5%. In the concentration study, three concentrations of loaded paclitaxel or Taxol® were tested: 0.25µg/mL, 2.5µg/mL and 25µg/mL. The cell viability of corresponding placebo nanoparticles was also tested as control. The incubation time for this study was 24 hours. For the time effect study, the drug concentration remained at 0.25µg/mL while the

incubation time varied from 24 hours to 72 hours. Placebo nanoparticles were also tested in the time effect study.

It is quite clear that with the increase of concentration and time, the cell viability decreases. Drug loaded nanoparticles showed a comparable effect in killing cancer cells of pure taxol® in the concentration and time intervals tested.

In the concentration effect study, C6 cells had about 80% viability at the concentration of 0.25μg/mL; when the drug concentration increased to 25μg/mL, this value decreased to about 60%, which indicated that concentration had much effect in cell viability. Similar trend has also been found by other groups using doxorubicin loaded PLGA microparticles (Lin et al., 2005). If the drug concentration goes to a too high value, the toxic adjuvant Cremophor EL of taxol® might also begin to kill cells and it will be hard to compare the effect of paclitaxel loaded nanoparticles and taxol®itself. Although drug loaded nanoparticles and pure taxol® showed comparable effect in killing C6 brain cancer cells, the particle formulation has more advantages considering only around 10% of the drug released from the particles in 24 hours in the *in vitro* release profile. This augment might be caused by the increased uptake percentage of the particles than pure taxol®. Due to the existence of P-gp, it is very difficult for pure drug to enter cells. However, the nanoparticle formulation can mask the characteristics of P-gp and easily enter the cells.

For the time effect study, similarly, cell viability was around 80% after incubating for 24 hours at the concentration of 0.25μg/mL. However, after 72 hours, cell viability decreased to only about 50% at the same concentration. It is thus can be seen longer time with even lower concentration may exert great effect on cell viability. This might be

caused by the release of paclitaxel from nanoparticles, especially in the first several days when the initial burst happens. We can also discover from the two figures that vitamin E TPGS emulsified nanoparticles have the relative lowest cell viability in different concentrations and time. The higher mortality of C6 cells to TPGS emulsified nanoparticles may be caused by the high cellular uptake of the drug loaded nanoparticles compared with other batches of nanoparticles and pure drug. The comparison of cellular uptake study will be discussed later. Moreover, the placebo PLGA nanoparticles with different emulsifiers all showed no cytotoxic effect on cells in this study, which indicated that it was the drug released not the nanoparticles themselves that killed the cells. All these results demonstrate paclitaxel loaded PLGA nanoparticles as a potential tool to treat brain cancers.

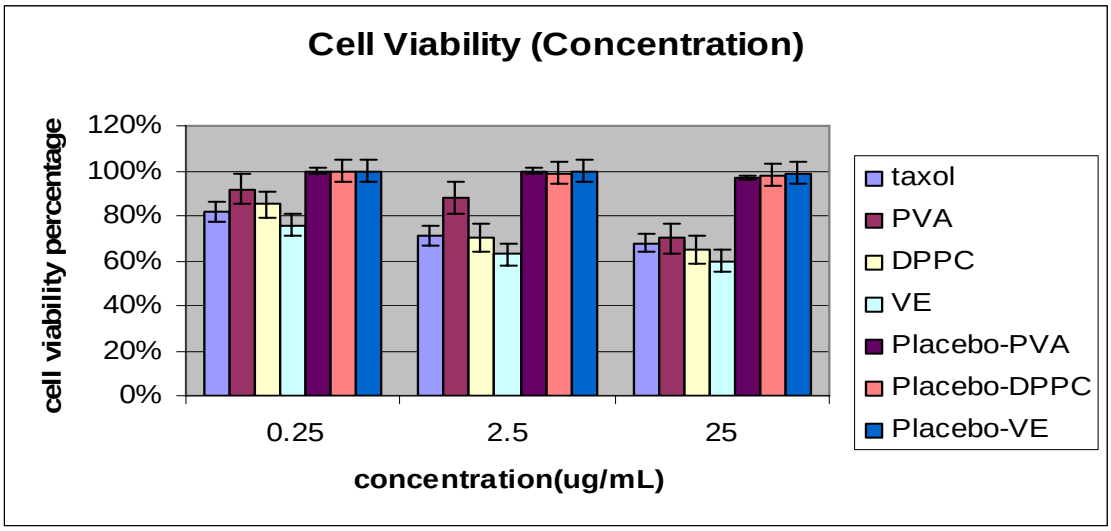

Fig 4.8 C6 cell viability study of pure taxol, 5% paclitaxel loaded and no drug loaded (placebo) PLGA nanoparticles with different emulsifiers in different concentrations, incubation time=24h. (n=6)

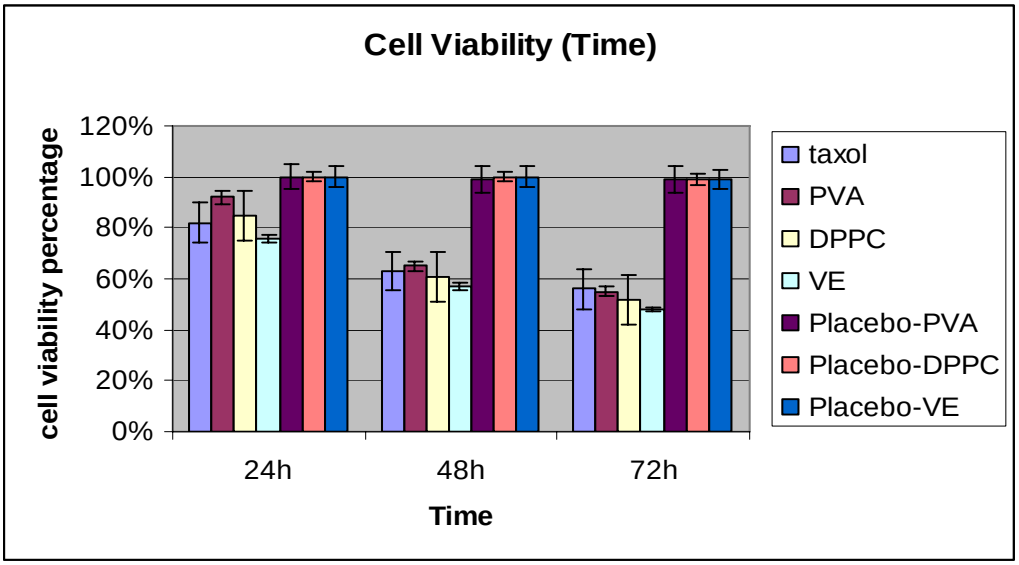

Fig 4.9 C6 cell viability study of pure taxol, 5% paclitaxel loaded and no-drug loaded (placebo) PLGA nanoparticles with different emulsifiers in different time intervals. Concentration=0.25 µg/mL (n=6)

Chapter 5

In Vitro and *In Vivo* Uptake Study of Fluorescence Loaded Polymeric Nanoparticles to Cross the Blood Brain Barrier

Blood brain barrier plays an important part in preventing the drug from entering the brain freely. The uptake experiment of fluorescent marker loaded nanoparticles through simple *in vitro* BBB model and *in vivo* can give direct evidence of nanoparticles' possible ability to enter the brain.

5.1 MDCK Cell Line as *In Vitro* BBB Model

In this project, MDCK (Madin-Darby canine kidney), a well characterized model for many biological functions, was used as the simple *in vitro* model of the blood brain barrier for cell uptake experiment. This cell line is endowed with the ability to form polarized monolayers that express tight junctions in the apical side. MDCK cells also produce many of the enzymes found in the brain endothelial cells. Under appropriate culture condition, monolayers with tightness comparable to that found in the brain endothelial cells can be obtained within days of culture. MDCK monolayers represent a relatively simple model for the screening of compounds that are transported passively across the blood-brain barrier. Although other systems such as the primary brain microvessel cells and co-culture system are also used in BBB investigation (Borchard et al., 1994), it is relatively difficult to maintain these systems compared with MDCK system. Fig 5.1 shows the morphology of MDCK cell line of about 80% confluence after

5 days' culture. This image was taken with the Olympus 1X700 optical microscope in chemotherapeutic engineering lab, NUS.

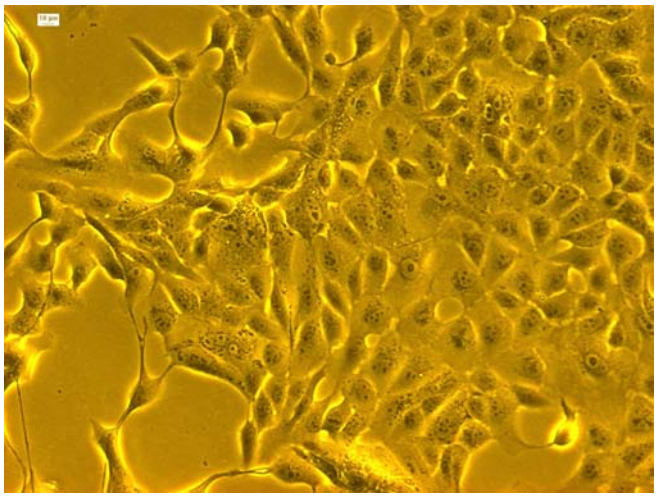

Fig 5.1 Morphology of MDCK cell line reaching ~80% confluence after ~5 days' culture

5.2 Cell Uptake Study

Cell uptake study is to validate the ability of nanoparticles to cross the *in vitro* BBB model. MDCK cell line was used as a simple simulation of the *in vitro* blood brain barrier in this experiment.

5.2.1 Surfactant Effect

In order to test the effect of emulsifiers on cellular uptake of nanoparticles, fluorescent marker coumarin-6 was encapsulated into the PLGA nanoparticles with different emulsifiers using single emulsion method. The resulting nanoparticles had similar particle size, size distribution and zeta potential to the paclitaxel loaded nanoparticles. The quantitative uptake percentage could be obtained via microplate reader.

To prevent the misinterpretation of nanoparticle uptake data due to the dissociation or leaching of coumarin-6 directly into the cells, *in vitro* release of fluorescent marker was also carried out using microplate reader within 24 hours. It was found that less than 0.5% of coumarin-6 released from all batches of nanoparticles during this period. Since the incubation time was only 4 hours in this experiment, so the released fluorescent marker can be neglected. Lu et al. also detected similar low release of coumarin-6 from nanoparticles *in vitro* with different pH buffers using fluorescent column HPLC (Lu et al., 2005). Moreover, the relative inertia of coumarin-6 encapsulated in PLGA nanoparticles guaranteed the dye not to leak out under the physiological conditions or under the acidic endo-lysosome compartment (Panyam et al., 2003). Actually, coumarin-6 encapsulated nanoparticles are widely used in cell uptake experiment (Khin and Feng, 2005; Davda and Labhasetwar, 2002; Panyam et al., 2002).

Fig 5.2 below shows the cell uptake percentage of PLGA nanoparticles with different emulsifiers after 4 hours' incubation with the particle concentration of 250μg/mL. Generally, 4 hours is enough for cells expressing brain structure to reach their highest uptake percentage (Ramge et al., 2000). 29.4% PVA emulsified nanoparticles were taken up by MDCK cells, the uptake percentage of DPPC&PVA emulsified nanoparticles was 41.0% and vitamin E TPGS emulsified nanoparticles exerted the highest uptake percentage of up to 63.8%, which was more than 2 folds of PVA emulsified nanoparticles. This difference in the uptake percentage is mainly caused by the surfactant on particle surface. PVA is a kind of chemical surfactant and the remaining PVA on particle surface may reduce the intracellular uptake because it makes the particle surface more hydrophilic, thus becomes difficult to interact with the hydrophobic cell membrane. On

the other hand, DPPC is a kind of natural lipid surfactant and DPPC coated nanoparticles are not only nontoxic but also help to enhance the cellular uptake since the lipid has similar structure as cell membrane. Fenart et al. reported similar research on phospholipids DMPC coated nanoparticles which showed enhanced ability to cross BBB without degradation (Fenart et al., 1999). For vitamin E TPGS emulsified nanoparticles, the remaining TPGS on particle surface formed a natural surfactant layer which not only had enhanced interaction with cells but also inhibited the P-glycoprotein on the MDCK membrane surface (Dintaman and Silverman, 1999). All of these can account for the highest cell uptake of TPGS emulsified nanoparticles.

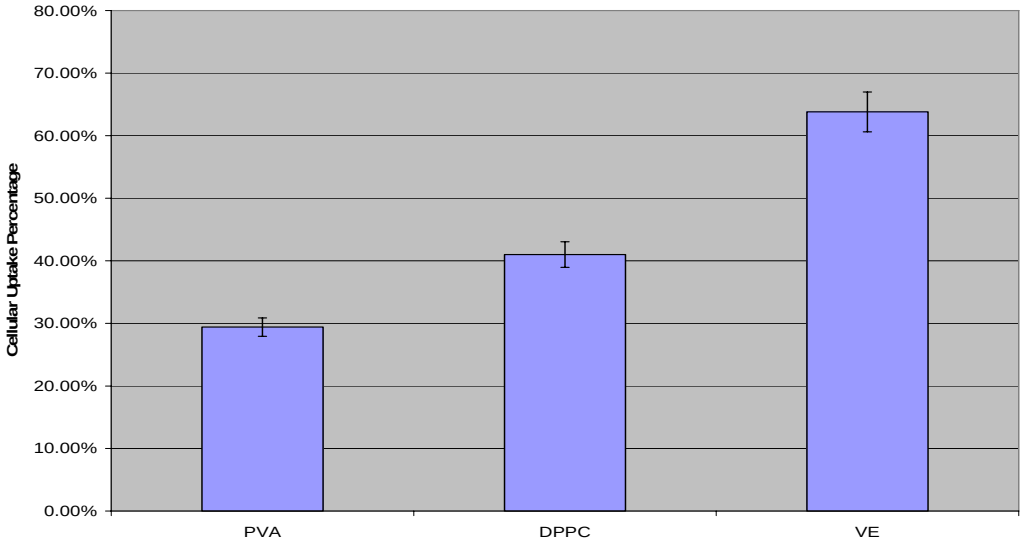

Fig 5.2 MDCK cellular uptake of PLGA nanoparticles with different emulsifiers, incubation time = 4 hours, concentration = 250 μg/mL. (n=6)

5.2.2 Particle Size Effect

Besides surfactant, particle size also plays a key role in adhesion and interaction with biological cells (Foster et al., 2001), especially for cells that express tight junctions such

as MDCK cell line used in this experiment. Although the PLGA nanoparticles showed favorable cellular uptake with their particle size within 200nm to 300nm, it is necessary to do further investigation on particle size effect so that we can develop more favorable nanoparticles for brain drug delivery. Commercial fluorescent polystyrene (PS) nanoparticles with various uniform sizes were used in this investigation. The tested sizes included 20nm, 57nm, 100nm, 200nm, 510nm. All particles had a negative surface charge. The incubation time for nanoparticles was also 4 hours. Three different concentrations: 50μg/mL, 250 μg/mL, 500 μg/mL were used to validate the result.

Fig 5.3 below showed the MDCK cellular uptake profile of different concentration PS nanoparticles with uniform sizes within 20nm~ 510nm. The fluorescent PS nanoparticles are suitable for the cell uptake study since the encapsulated fluorescence also releases very slowly and would not cause false reading (Kin and Feng, 2005). Obviously, the cell uptake percentage of PS nanoparticles was much lower than PLGA nanoparticles. The highest cellular uptake of PS nanoparticles was only about 16%. This should mainly be caused by different characteristics of the two polymers. Unlike PLGA, PS, which is often used to produce plastic bags, is not biodegradable or biocompatible. However, PS can produce nanoparticles with various uniform sizes, especially very small sizes, so it also has wide application in scientific research. Another reason for the low uptake of PS nanoparticles might be the lack of proper surfactant on particle surface.

From Fig 5.3, we can see in the whole concentration range, the 57 nm PS nanoparticles showed the highest uptake percentage and 20nm, 500nm nanoparticles showed the lowest uptake percentage compared with other sizes. 100nm and 200nm nanoparticles showed

quite similar uptake percentage which was between the highest and the lowest. The results implied particle size around 60nm may have the best uptake percentage by cells expressing tight junctions. This might be caused by the combination of several mechanisms to uptake particles of this size including paracellular passage, endocytotic uptake and phagocytosis. It has been reported that phagocytic uptake took place with a cut-off size of about 500nm. For nanoparticles of lower size, they can also be taken up by fluid phase endocytosis (Suh et al., 1998; Foster et al., 2001). Particle size of 500nm or above might be too large for drug delivery to brain. The surprisingly low uptake percentage of the 20nm nanoparticles might be caused by the aggregation of the particles due to their too small size. The result of the experiment showed that particle size for brain delivery was not necessarily the smaller, the better. An optimal particle size is very important for cellular uptake.

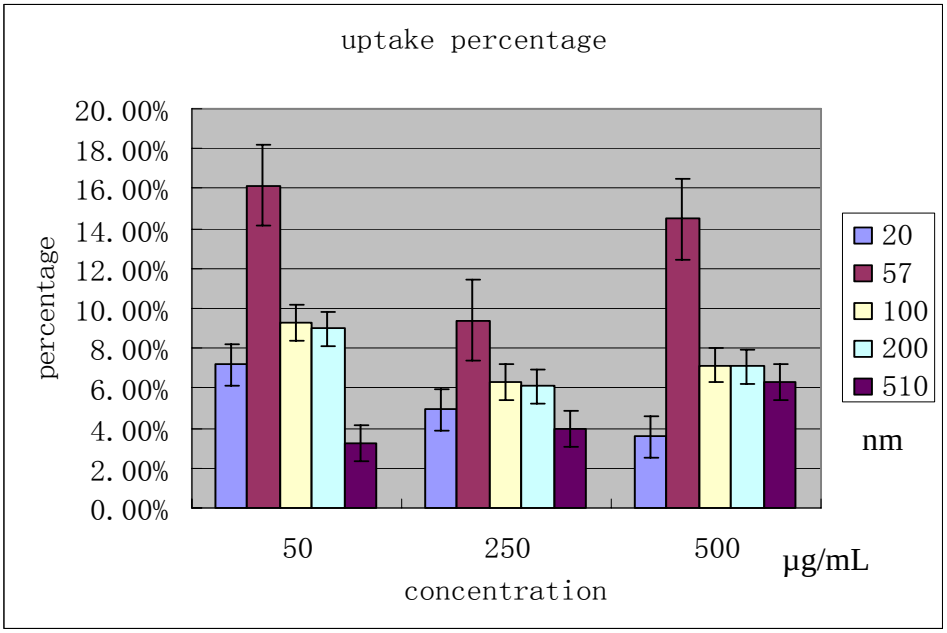

5.3 MDCK cellular uptake profile of fluorescent polystyrene nanoparticles with uniform particle sizes (n=6), the concentration unit is μg/mL, the size unit is nm.

5.3 Confocal Study

From above studies, the cellular uptake percentage of PLGA nanoparticles with different emulsifiers was investigated quantitatively using microplate reader. To give direct evidence that nanoparticles had really come into the cells instead of just attaching to them, confocal laser scanning microscopy was used to visualize the internalization of nanoparticles. Fig 5.4 below shows the confocal images of nanoparticles into MDCK cell line. The nuclei of cells were stained red with PI (propidium iodide) while the nanoparticle had a fluorescence of green. We can see from the pictures that most nanoparticles had internalized the cytoplasma of the cells and vitamin E TPGS emulsified nanoparticles had the thickest layer of drugs internalized. No fluorescence could be detected by the control cells not exposed to coumarin-6 loaded nanoparticles and the placebo nanoparticles, which meant no false reading was caused by auto fluorescent of the cells or the polymers.

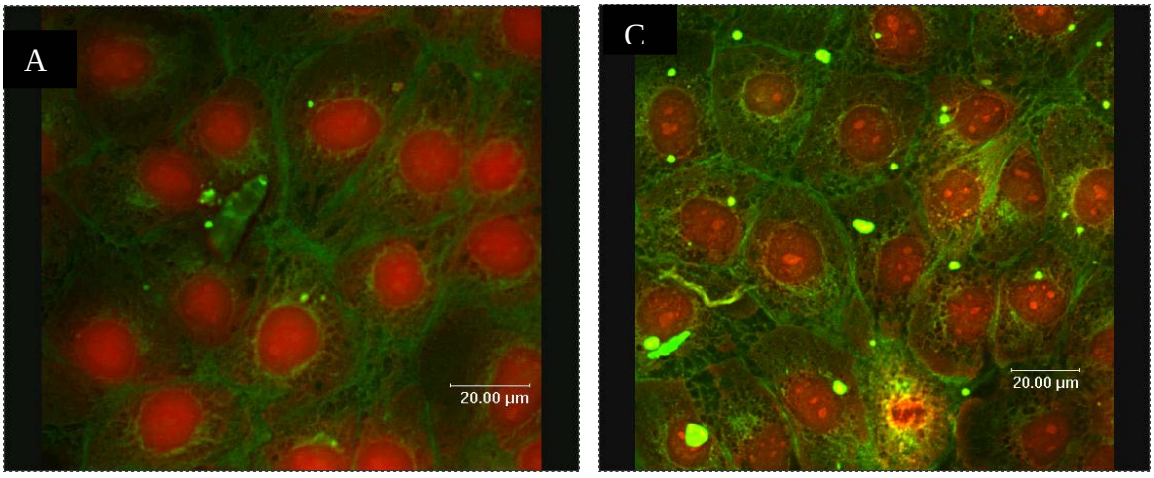

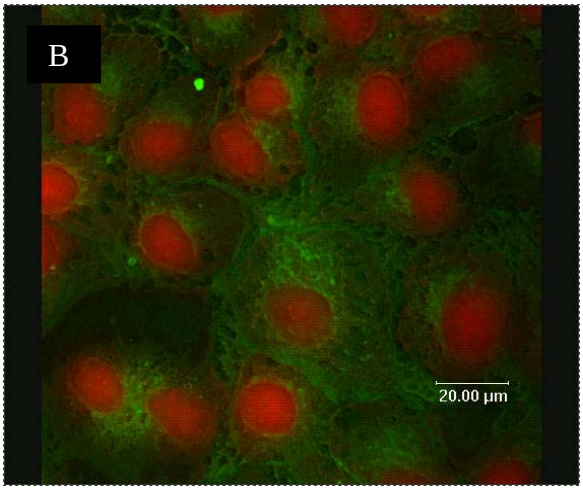

Fig 5.4 Confocal images of fluorescence loaded PLGA nanoparticles with different emulsifiers. (a) PVA emulsified nanoparticles (b) DPPC& PVA emulsified nanoparticles (c) vitamin E TPGS emulsified nanoparticles

5.4 *In Vivo* Study with Rat Models

Although *in vitro* studies have shown great potential for PLGA nanoparticles to cross the blood brain barrier, it is necessary to carry out *in vivo* study to validate this assumption. Male Sprague Dawley rats of around 200g in weight were used as animal model. From previous study, we can see all batches of nanoparticles had favorable characteristics, of which vitamin E TPGS emulsified PLGA nanoparticles had the best cellular uptake *in vitro*, so it was used as model nanoparticles. Coumarin-6 was used as fluorescent marker due to its relative inertial property in physiologic environment and very low release rate mentioned previously (Panyam et al., 2003). It is also reported that polysorbate coating on nanoparticles plays a very important role in brain targeting and polysorbate 20, 40, 60, 80, 85 (tween 20, 40, 60, 80, 85) are the only kinds of surface coating that can effectively help nanoparticles across the blood brain barrier *in vivo* (Kreuter, 2001). Thus the model

PLGA nanoparticles were overcoated with tween 80 and centrifuged to remove excess coatings before injecting to the animal models. 0.3 mL nanoparticle suspension in 0.9%(w/v) NaCl saline was injected intravenously to the rat tail. After 90 minutes, rats were killed and their residual blood was rinsed before their brains were fixed and cut into tissue slices. Besides tween 80 coated PLGA nanoparticles, naked PLGA nanoparticles and pure saline were also injected to control rat groups. No mortality of rats was observed after injection of coumarin-6 loaded PLGA nanoparticles, which indicated the safety of using PLGA nanoparticles as drug carriers.

The prepared brain tissue slices were observed under fluorescence microscope. Tween 80 coated PLGA nanoparticles had significant fluorescence as shown in Fig 5.5 while the control groups of pure saline and naked PLGA nanoparticles injected in rat brain tissues showed no fluorescence under the same fluorescence intensity and exposure time. This indicates that the rat brain tissue has no or very weak auto-fluorescence and tween 80 is very important in brain targeting and crossing BBB. This result is quite correspondent with researches of Sun et al. who investigated the FITC-dextran loaded PLA nanoparticles to cross the BBB *in vivo* (Sun, et al., 2004). From Fig 5.5, it was quite clear the blood vessels of rat brain had more fluorescence. This is easy to understand since the particle solution was injected through venous vessels. We can also find that the surrounding brain tissues were stained, which indicated the potential of nanoparticles across the blood brain barrier and migrated from the 'blood' to the 'brain'. Our study gave direct evidence of fluorescence-loaded PLGA nanoparticles to be delivered to the brain intravenously and had the potential to cross the blood brain barrier.

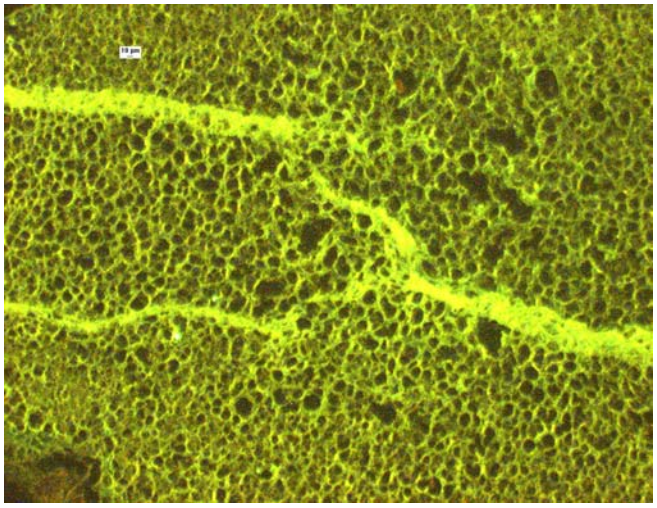

Fig 5.5 Fluorescence microscope image rat brain tissue after injection with tween-80 coated PLGA nanoparticles. (bar =10μm)

Chapter 6

Formulation and Characterization of Gadolinium-DTPA Encapsulated Nanoparticles for Potential In Vivo Imaging

6.1 Significance to Develop MRI Contrast Agent Gd-DTPA Encapsulated Biodegradable Nanoparticles

In previous studies, we used invasive histological method of tissue analysis to investigate the potential of nanoparticles to cross the blood brain barrier *in vivo* by injecting fluorescent marker loaded nanoparticles intravenously and observing the resulting brain tissue slice directly under fluorescence microscope. Other indirect methods such as tail flick (Alyautdin et al., 1997), hot plate (Schroeder et al., 1998) have also been adopted by other groups. However, all these methods can not continuously assess the delivery and distribution of particles *in vivo*. Thus it is necessary to develop a kind of noninvasive and continuous monitoring technique to evaluate the *in vivo* behavior of nanoparticles. Due to its high spatial and temporal resolution, magnetic resonance imaging (MRI) becomes a good candidate for non-invasive imaging. To enhance the MR images' contrast, various contrast agents are often used, of which the chelated paramagnetic gadolinium Gd-DTPA is the most widely adopted due to its good effect and low toxicity. By encapsulating the MRI contrast agent into the nanoparticles of biodegradable polymers, we can thus have the potential to achieve the monitoring of local drug delivery and release kinetics *in vivo*. And this would also greatly enhance the value of particle based drug delivery systems

(Chen et al., 2005). The following investigations tested the feasibility of encapsulating Gd-DTPA into biodegradable nanoparticles and their MRI characteristics *in vitro*.

6.2 Size, Size Distribution, Zeta Potential Study

Table 6.1 Size, size distribution and surface charge of Gd-DTPA encapsulated nanoparticles with various formulations

Type	Size (nm)	polydispersity	zeta potential(mV)
PLGA(NP*)	398.3	0.230	-18.95
PLGA(DE*)+TPGS	3000.0	0.085	-20.34
PLGA(DE*)+PVA	269.0	0.073	-17.13
PLGA +salt(NP*)	234.4	0.209	-15.15
MPEG-PLA(NP*)	106.2	0.161	-15.04
MPEG-PLA(DE*)	252.3	0.142	-14.31

* DE= double emulsion, NP=nanoprecipitation

Table 6.1 summarized the particle size, size distribution and surface charge of Gd-DTPA encapsulated nanoparticles. Double emulsion and nanoprecipitation methods were used to encapsulate the hydrophilic Gd-DTPA. Besides PLGA, MPEG-PLA with PEG ratio of 10% was also used since the existence of PEG chains made the co-polymer more hydrophilic and have better interactions with Gd-DTPA. Different emulsifiers PVA and vitamin E TPGS were also tried.

Unlike single/double emulsion, the process of nanoprecipitation doesn't need any emulsifiers to form the nanoparticle droplets. The Gd-DTPA encapsulated PLGA nanoparticles using nanoprecipitation had a relative larger particle size than other batches

of nanoparticles. However, after adding some salt such as Na_2HPO_4 in the water phase during the fabrication process, the particle size decreased a lot. This may be caused by the added ions and the changed pH in aqueous phase (Govender et al., 1999, Peltonen et al., 2004). Compared with PLGA, Gd-DTPA encapsulated MPEG-PLA nanoparticles had much smaller particle size of around 100nm. Dong and Feng also reported small particle size of paclitaxel loaded MPEG-PLA nanoparticles using nanoprecipitation (Dong and Feng, 2004). The smaller particle size is favorable for the purpose of crossing blood brain barrier just as discussed above.

From table 6.1, we can also find emulsifiers play an important role in determining the particle size in the double emulsion methods, even more significant than in single emulsion. For PVA emulsified PLGA nanoparticles, the size was 269.0nm, which was comparable with the size of nanoparticles using single emulsion we developed previously. However, for vitamin E TPGS emulsified PLGA nanoparticles using double emulsion, the size was as much as 3μm. Just as discussed previously, this should be caused by the relative low molecular weight of TPGS, which makes it less efficient to form smaller particle size.

The size distribution of all batches of nanoparticles varied from 0.073 to 0.230. Generally, double emulsion method resulted in a smaller size distribution than nanoprecipitation.

We can also see from table 6.1 that all batches of nanoparticles had a negative surface charge and MPEG-PLA nanoparticles had smaller negative charge than PLGA nanoparticles. This might be caused by the presence of more carboxyl groups of PLGA at the particle surface.

6.3 Morphology of Gd-DTPA Encapsulated Nanoparticles

FESEM pictures were taken to give a direct and close observation of the nanoparticles. Compared with SEM, FESEM has higher resolution and can give clearer image of samples with small particle size. Fig 6.1 showed the FESEM images of Gd-DTPA encapsulated PLGA and MPEG-PLA nanoparticles using double emulsion method or nanoprecipitation method. The FESEM confirmed the results of laser light scattering (LLS) that MPEG-PLA nanoparticles using nanoprecipitation had small particle size around 100nm. For other batches, the particle sizes were between 200~400nm. All batches of nanoparticles had spherical shape. However, some particles, such as the PLGA nanoparticles using double emulsion showed a sticky state, which might be caused by the aggregation of particles. For MPEG-PLA nanoparticles using double emulsion, there seemed to be some foggy things around the nanoparticles. This might be the Gd-DTPA on or near the surface of the nanoparticles, since most of the hydrophilic PEG chain was on the surface of the nanoparticles.

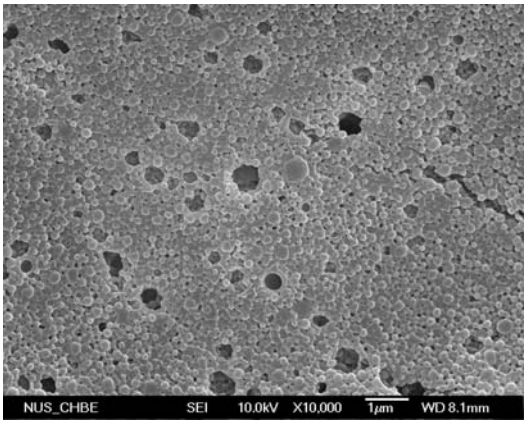

(a)

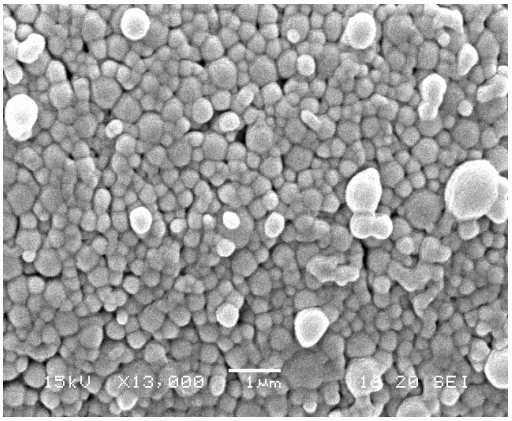

(b)

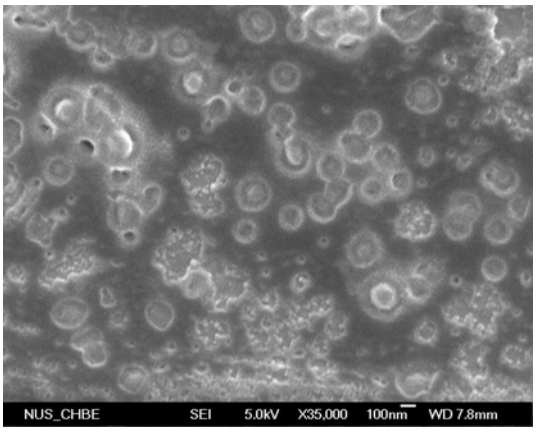

(c)

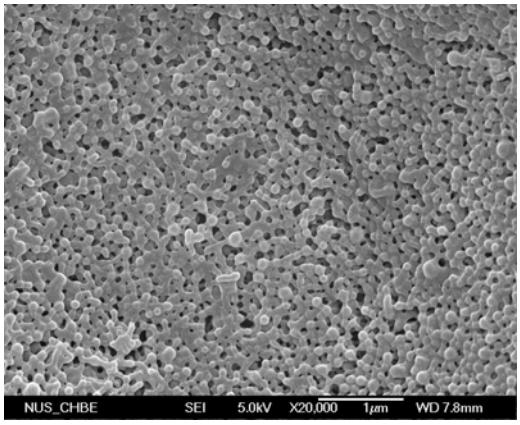

(d)

Fig 6.1 FESEM images of Gd-DTPA encapsulated nanoparticles.(a) PLGA nanoparticles using double emulsion, bar=1μm (b) PLGA nanoparticles using nanoprecipitation, bar=1μm (c) MPEG-PLA nanoparticles using double emulsion, bar=100nm (d)MPEG-PLA nanoparticles using nanoprecipitation, bar=1μm

6.4 Drug Entrapment and *In Vitro* Release Profile of Gd-DTPA Encapsulated Nanoparticles

6.4.1 Drug Entrapment Study

Table 6.2 Drug entrapment of Gd-DTPA encapsulated nanoparticles with various formulations

Type	Drug Entrapment (%)
PLGA(NP*)	<0.5
PLGA(DE*)+TPGS	1.51
PLGA(DE*)+PVA	0.64
PLGA +salt(NP*)	<0.5
MPEG-PLA(NP*)	0.96
MPEG-PLA(DE*)	1.32

One of the limiting factors to develop nanoparticle based drug carriers is the low encapsulation efficiency and drug entrapment. Drug entrapment is an important parameter since higher drug entrapment could help to decrease the dose of nanoparticles used for further *in vivo* experiment. In this experiment, ICP-OES was used to measure the content of Gd-DTPA in nanoparticles. Table 6.2 summarizes the drug entrapment of Gd-DTPA encapsulated nanoparticles. All of them showed very low entrapment. Due to the large amount of Gd-DTPA used during fabrication (45mg Gd-DTPA with 75 mg polymer), the encapsulation efficiency for all batches was also very low (<3%). For PLGA nanoparticles fabricated by nanoprecipitation, the entrapment was too low (<0.5%) and did not have meanings in further application. When drug loaded PLGA nanoparticles were fabricated with double emulsion, the drug entrapment increased. Vitamin E TPGS emulsified PLGA nanoparticles had the drug entrapment of 1.51%, meaning 100mg nanoparticles had 1.51mg drug encapsulated. However, considering the size of the particle, which was about 3μm, it is not suitable to develop this kind of particles for monitoring their BBB crossing kinetics. For MPEG-PLA nanoparticles, the drug entrapment was higher than that of PLGA nanoparticles with comparable or even smaller particle size. Thus the following experiments would be based on Gd-DTPA encapsulated MPEG-PLA nanoparticles using double emulsion or nanoprecipitation.

In order to find out the loss of Gd-DTPA in the process of centrifugation, the content of Gd-DTPA in the surpernatant was also measured using ICP-OES. For all samples, in the first wash, around 80% Gd-DTPA was lost in the supernatant instead of being encapsulated into the polymer matrix. This might be caused by the hydrophilicity of Gd-DTPA, thus hard to be encapsulated or just adhered to the particle surface loosely. In the

subsequent washes, the supernatant contained much smaller amount of free Gd-DTPA than the first wash, which was less than 3%. Other loss of Gd-DTPA might happen during the fabrication process. From these results, we can see that the later two washes of nanoparticles can not be skipped in order to guarantee most of the Gd-DTPA was encapsulated in the polymer matrix instead of attaching to the surface.

6.4.2 *In Vitro* Release Kinetics

In vitro release of Gd-DTPA from MPEG-PLA nanospheres was investigated in PBS solution (pH=7.4) at 37^{o}C in an orbital shaker. This experiment was carried out within 48 hours. The Gd-DTPA encapsulated MPEG-PLA nanoparticles, which were fabricated by either double emulsion or nanoprecipitation, were chosen to take the *in vitro* release test since they had relative higher drug entrapment and favorable particle size.

Both of the particles showed sustained release with an initial burst as shown in Fig 6.2. The initial burst might be caused by the relative easy release of Gd-DTPA near or on the particle surface. It is obvious that nanoparticles using double emulsion (DE) had a slower release rate than nanoparticles using nanoprecipitation (NP). For DE nanoparticles, less than 40% Gd-DTPA was released at the end of 48 hours while this value for NP nanoparticle was more than 50%. The reasons might be that MPEG-PLA nanoparticles fabricated by nanoprecipitation had much smaller particle size than particles by double emulsion. The smaller particles had higher surface area to volume ratio, thus could have a higher release rate.

Overall, Gd-DTPA encapsulated MPEG-PLA nanoparticles showed favorable release profile. However, the release kinetics might be different in *in vivo* situation since many enzymes exist in the body which can cut off the polymer chain and speed the release rate.

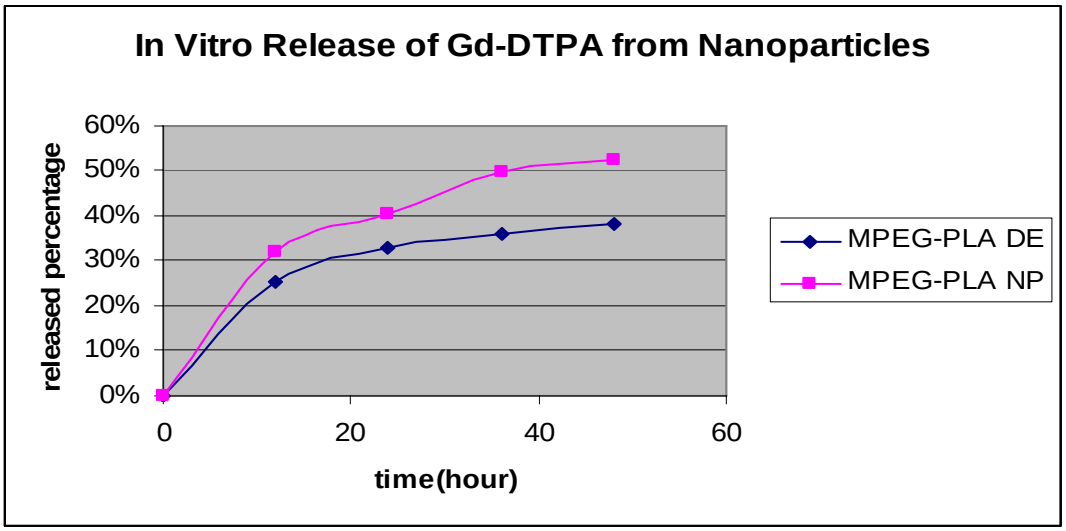

Fig 6.2 *In vitro* release profile of Gd-DTPA encapsulated MPEG-PLA nanoparticles. DE=double emulsion, NP=nanoprecipitation.

6.5 MRI Characterization

Gd-DTPA encapsulated nanoparticles were detected and differentiated by MRI. The MRI study was carried out on a 1.5 T scanner with a head coil. Since Gd-DTPA is a kind of T1-weighted positive contrast agent, T1 relaxation time was measured and converted to the R1 relaxation rate, which equals to 1/T1.

6.5.1 Calibration Curve of pure Gd-DTPA *In Vitro*

T1 relaxation time of pure Gd-DTPA in different concentrations were measured and converted to R1 relaxation rate to produce the calibration curve. The Gd concentration

was ranging from 0 to 0.2mM. Inversion recovery gradient-echo images were acquired to measure T1. The imaging parameters were set as follows: slide thickness=5mm, TR= 25-6400 ms and TE=12ms. Fig 6.3 shows the calibration curve of Gd-DTPA dissolved in water. The six concentrations can be fit into a straight line with high linear correlation coefficient of up to 0.9981 and the equation to describe the line was y=4.0077x+0.3148, where x is the Gd concentration in millimole/liter and y is the R1 relaxation rate in s^{-1}. The slope 4.007 is actually the relaxivity of the contrast agent.

Although dispersing Gd-DTPA in water is the simplest way to have the MRI test, water can not mimic the characteristics of tissues well and nanoparticles can settle down in water after a period of time which will make the measurement difficult. Therefore Gd-DTPA was dispersed in 8% gelatin (w/v) to make another calibration curve and compared with the calibration curve which dissolved Gd-DTPA in water. Gelatin can not only help to make the nanoparticles evenly distributed in subsequent experiments but also can mimic the tissues better. From Fig 6.4, we can see after being dispersed in the gelatin gel, the concentration of Gd and R1 relaxation rate still have a linear relationship. The linear correlation coefficient was also very high of up to 0.9991. The equation to describe the relationship was y=4.9229x+0.716. We can discover the relaxivity of Gd-DTPA in gelatin is higher than that in water.

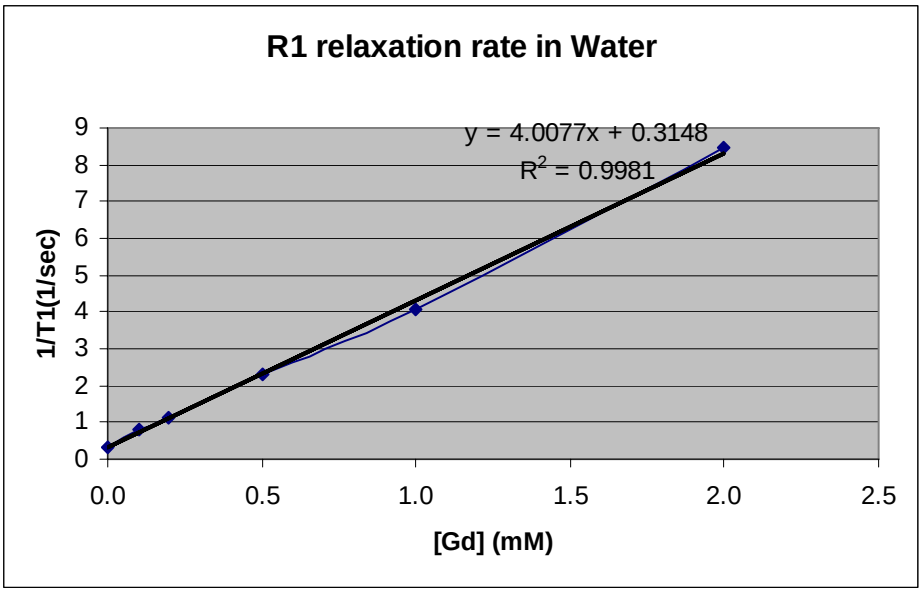

Fig 6.3 Calibration curve of Gd concentration to R1 relaxation rate in water using pure Gd-DTPA

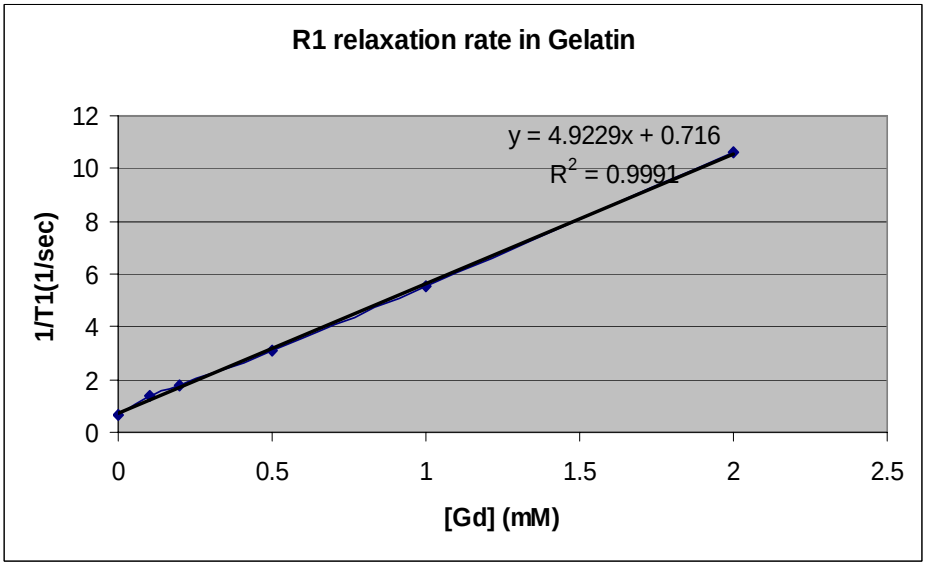

Fig 6.4 Calibration curve of Gd concentration to R1 relaxation rate in gelatin using pure Gd-DTPA

6.5.2 Relaxation Rate Characteristics of Gd-DTPA Encapsulated Nanoparticles

The R1 relaxation rate of Gd-DTPA loaded nanoparticles was investigated to study the effect of polymer encapsulation. Nanoparticles in both water and gelatin are investigated. Gd-DTPA encapsulated nanoparticles were dispersed in the water and gelatin at the concentration of 40mg/ml. T1 was measured using the same MRI parameters as mentioned above. T1 relaxation time of pure water and blank nanoparticles were also measured and converted to R1 relaxation rate. From Fig 6.5, we can discover that pure water and blank MPEG-PLA nanoparticles without any drugs had a very low relaxation rate compared with Gd-DTPA encapsulated nanoparticles. Therefore the R1 relaxation rate of drug loaded nanoparticles is mainly caused by the Gd-DTPA encapsulated. Using the calibration curve above, the relaxation rate can be converted to the Gd concentration. For nanoparticles fabricated by nanoprecipitation, the converted Gd concentration was 0.363mM and for nanoparticles by double emulsion, the converted concentration was 0.684mM. However, considering the drug entrapment which was measured by ICP-OES, the Gd concentration for nanoprecipitation and double emulsion nanoparticles should be 0.70mM and 0.96 mM, respectively. This result showed that after encapsulating into the polymer matrix, the R1 relaxation rate of Gd-DTPA decreased. This reduction in R1 relaxation rate might be caused by the shielding effect of the polymer. Encapsulated Gd-DTPA was prevented by the surrounding polymer from interacting with the hydrogen atoms.

Just as mentioned previously, gelatin gel can simulate the tissue characteristics and help to prevent the nanoparticles from settling down. 8% gelatin (w/v) was prepared to embed the nanoparticles as described by Faranesh et al.(Faranesh et al., 2004) . From Fig 6.6, we can see pure gelatin and blank polymeric nanoparticles in gelatin also exerted only small relaxation rate, although it was larger than that of water. The R1 relaxation rate of pure gelatin was similar to the value reported by Chen et al. (Chen, et al., 2005). In the same way, the R1 relaxation rate can be converted to Gd concentration using the calibration curve. For nanoprecipitated and double emulsified nanoparticles, the converted concentration was 0.267mM and 0.413mM, respectively. It is also smaller than the actual concentration of encapsulated Gd-DTPA measured by ICP-OES previously (0.70mM for nanoprecipitated MPEG-PLA nanoparticles and 0.96 mM for double emulsified MPEG-PLA nanoparticles). This also might be caused by the shielding effect of the polymer. Fig 6.7 shows the MRI images of the Gd-DTPA encapsulated MPEG-PLA nanoparticles and the blank nanoparticles both in water and in gelatin.

From these experiments, we can conclude that positive MRI contrast agent Gd-DTPA can still exert their effect after being encapsulated into the biodegradable polymers. However, after encapsulating, their R1 relaxation rate decreased due to limited access of water to the contrast agent.

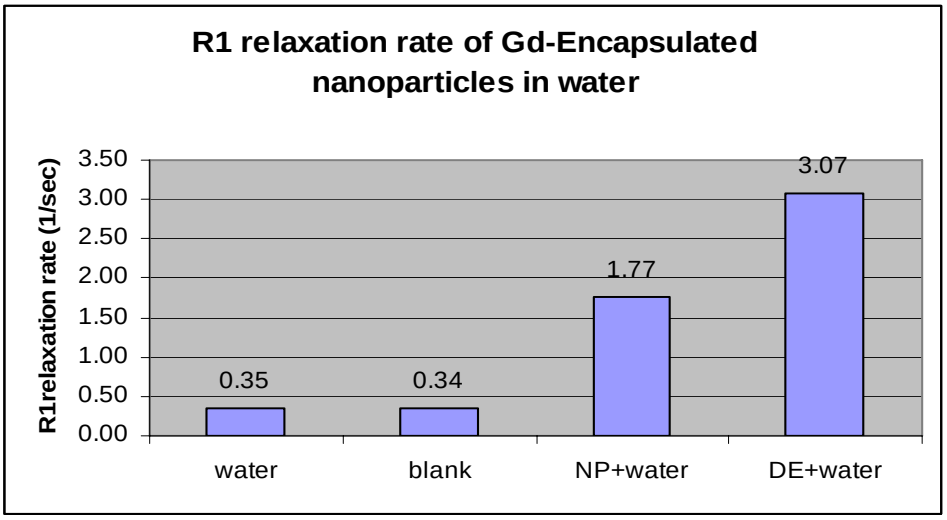

Fig 6.5 R1 relaxation rate of water, blank MPEG-PLA nanoparticles without Gd-DTPA, Gd-DTPA encapsulated nanoparticles using nanoprecipitation and Gd-DTPA encapsulated nanoparticles using double emulsion suspended in water

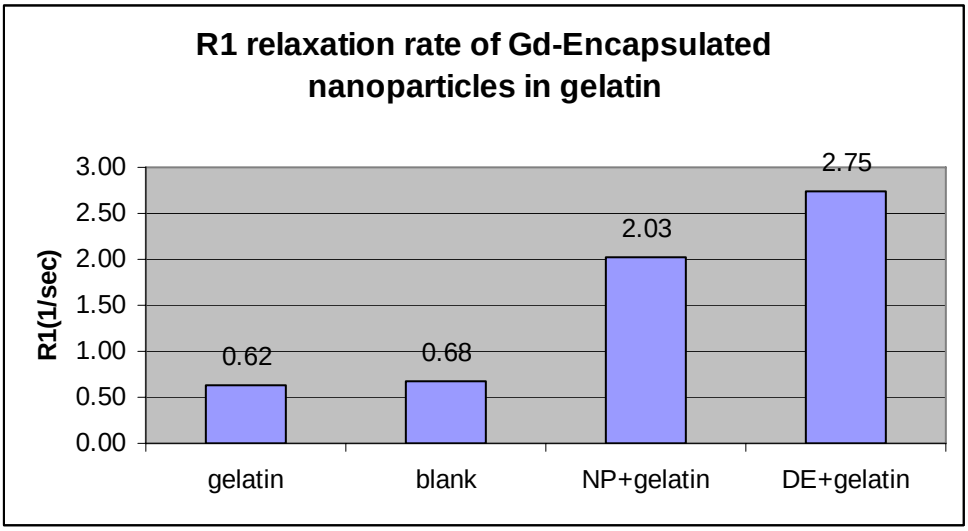

Fig 6.6 R1 relaxation rate of gelatin, blank MPEG-PLA nanoparticles without Gd-DTPA, Gd-DTPA encapsulated nanoparticles using nanoprecipitation and Gd-DTPA encapsulated nanoparticles using double emulsion suspended in gelatin

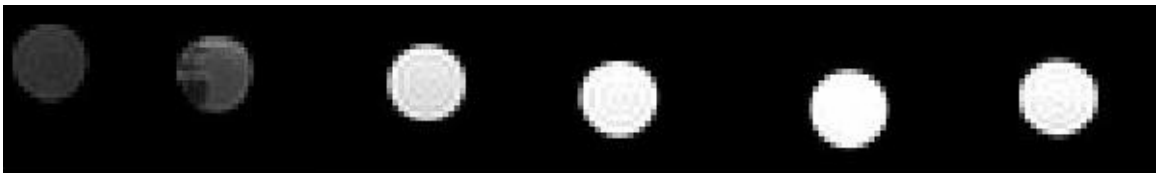

Fig 6.7 MRI images of Gd-DTPA encapsulated MPEG-PLA nanoparticles, from left to right: 1. blank nanoparticle in water, 2. blank nanoparticles in gelatin, 3. Gd-DTPA loaded nanoparticles using nanoprecipitation in water, 4. Gd-DTPA loaded nanoparticles using nanoprecipitation in gelatin, 5. Gd-DTPA loaded nanoparticles using double emulsion in water, 6. Gd-DTPA loaded nanoparticles using double emulsion in gelatin. TR= 800ms; TE =12ms, 256x256, 0.7mm in-plane and 5mm slice thickness

The above experiments investigated the *in vitro* characteristics of MRI contrast agent Gd-DTPA encapsulated nanoparticles of biodegradable polymers. The particle size, drug entrapment, *in vitro* releases and MRI effect were tested. These particles have favorable characteristics and can be used for further *in vivo* investigation.

Chapter 7

Conclusions and Recommendations

7.1 Conclusions

In this study, we investigated the feasibility of biodegradable PLGA nanoparticles to treat brain cancer and cross the blood brain barrier both *in vitro* and *in vivo*. Paclitaxel, a widely used anti-cancer drug was used as the model drug. The emphasis was put on the effect of emulsifiers and surfactants of the nanoparticle formulation. Two natural surfactants, DPPC and vitamin E TPGS were used and compared with the traditional chemical surfactant PVA. It was found that all batches of nanoparticles had a favorable particle size ranging from 245.2nm to 282.8nm. They also had a narrow size distribution and negative surface charge. SEM and AFM images revealed that all batches of nanoparticles had smooth surface morphology. Moreover, encapsulation efficiency (EE) experiment showed that vitamin E TPGS emulsified nanoparticles had a very high EE value of 92.30% while the EE values for PVA and DPPC emulsified nanoparticles were 58.42% and 45.71% respectively. Our *in vitro* release study demonstrated that PVA emulsified nanoparticles showed the fastest release rate of up to 68% while vitamin E TPGS emulsified nanoparticles only released about 40% drug during 25 days. Then cell viability study was carried out by employing rat glioma cell C6 as the model cancer cell line. It was revealed that compared with pure taxol®, paclitaxel loaded nanoparticles had comparable effect to kill cancer cells. Our results also showed that both time and

concentration had effects on the cell viability to drug loaded nanoparticles and pure taxol®. Longer time and higher concentration would result in less cell viability.

Fluorescent marker coumarin-6 was incorporated into the PLGA nanoparticles with various emulsifiers to carry out the cellular uptake study on MDCK cell line which was used as a simple *in vitro* BBB model. It was found that vitamin E TPGS emulsified nanoparticles had the highest cell uptake concentration of 63.8%, which was more than two folds of the PVA emulsified nanoparticles. Confocal microscopy was also carried out to give direct evidence of the internalization of nanoparticles to the cells. On the other hand, commercial fluorescent polystyrene nanoparticles with uniform sizes ranging from 20nm to 500nm were used to test the size effect on cell uptake. It was found that the 50nm nanoparticles had the highest uptake percentage by MDCK cell lines. Finally, after over coated with tween 80, the fluorescent PLGA nanoparticles were injected into rat from tail vein and the brain tissues were cut to slices to observe under fluorescence microscope. Fluorescence was observed both in blood vessels and surrounding tissues in the brain, which indicated PLGA nanoparticles had the potential to cross BBB *in vivo* with proper emulsifiers and surface coatings.

MRI contrast agent Gd-DTPA encapsulated biodegradable nanoparticles have also been developed for future noninvasive *in vivo* imaging. MPEG-PLA was used to fabricate nanoparticles using both double emulsion and nanoprecipitation since they exerted favorable size of 100~300nm and relative higher drug entrapment. *In vitro* release was also carried out within 48 hours and about 40% gadolinium was released out. MRI characterization revealed that both longitudinal and transverse relaxation rate of the Gd-

DTPA encapsulated nanoparticles were reduced compared with same amount of pure Gd-DTPA, which might be caused by the reduced access of water to the contrast agent.

7.2 Recommendations

In previous study, we used MDCK cell line as a simple BBB model to investigate the uptake experiment, furthermore, we should use more accurate model such as the co-culture system to clarify the mechanism of the particles getting out of the endothelial cells of the brain vessels and entering the brain parenchyma. We have also demonstrated qualitatively with histological tissue analysis that it is possible for biodegradable PLGA nanoparticles with proper emulsifiers and surface coatings to cross the blood brain barrier in rat models. In the future, quantitative bio-distribution study of model drug (such as paclitaxel) loaded nanoparticles in animals should be tested.

We have also had preliminary research on MRI contrast agent Gd-DTPA encapsulated nanoparticles for potential *in vivo* imaging. The study so far has been done *in vitro*. The *in vivo* imaging should be carried out in the future study.

REFERENCE

Alyautdin, N.R., Petrov, E.V., Langer, K., Berthold, A., Kharkevich, A.D., Kreuter, J. (1997). Delivery of loperamide across the blood-brain barrier with polysorbate 80-coated polybutylcyanoacrylate nanoparticles. *Pharm Res*, 14, 3, 325-328.

American Cancer Society. *Cancer facts & Figures*, 2005.

BBB History: http://users.ahsc.arizona.edu/davis/bbbhistory.htm

Beck, L.R., Pope, V.Z., Flowers, C.E., Cowsar, D.R., Tice, T.R., Lewis, D.H., Dunn, R.L., Moore, A.B. and Gilley, R.M.(1983). Poly(DL-Lactide-co-glycolide)/ norethisterone microcapsules an injectable biodegradable contraceptive. *Biol Reprod*, 28, 186.

Begley, D.J. (1996). The blood-brain barrier: principles for targeting peptides and drugs to the central nervous system. *J Pharm Pharmacol*, 48 (2), 136-46.

Betz, A. L. (1992). An overview of the multiple functions of the blood-brain barrier, in Bioavailability of Drugs to the Brain and the Blood-Brain Barrier, National Institute on Drug Abuse, Research Monograph Series.

Borchard, G., Audus, K.L., Shi, F., Kreuter, J. (1994). Uptake of surfactant-caoted poly(methyl methacrylate)- nanoparticles by bovine brain microvessel endothelial cell monolayers. *Int J Pharm*, 110, 29-35.

Borchardt, G., Audus, K.L., Shi, F. (1994). Uptake of surfactant-coated

poly-methyl-methylacrylate nanoparticles by bovine brain microvessel endothelial cell monolayers. *Int J Pharmaceutics*, 1994, 110, 29-35.

Boury, F., Ivanova, T., Panaiotov (1995). Dynamic properties of poly (D,L-lactide) and polyvinyl alcohol monolayers at the air/water and dichloromethane air/water interfaces. *J Colloid Interf Sci* 169, 380-392.

Brightman, M. W., Reese, T.S. (1969). Junctions between intimately apposed cell membranes in the vertebrate brain. *J Cell* Biol, 40, 648-677.

Bushong, C.S. (2003). Magnetic resonance imaging: physical and biological principles. pp. 65-72, Texas: Mosby, Inc.

Carrio, A., Schwach, G., Coudane, J., Vert, M. (1991). Preparation and degradation of surfactant-free PLGA microspheres. *J Control Release*, 37, 113-121.

Chen, H.H., Visage, C.L., Qiu, B., Du, X., Ouwerkerk, R., Leong, W.K., Yang, X., (2005). MR imaging of biodegradable polymeric microparticles: a potential method of monitoring local drug delivery. *Magnet reson med,* 53, 614-620.

Chen,Y., Dalwadi, G. and Benson, H.A.E. (2004). Drug Delivery Across the Blood-Brain Barrier. *Current drug delivery*, 1, 361-376.

Couvreur, P., Kante, B., Roland, M., Goit, P., Bauduin, P.,& Speiser, P.(1979). Polycyanoacrylate nanocapsules as potential lysosomotropic carriers: preparation, morphology and sorptive properties. *J Pharm Pharmacol*, 31, 331-332.

Cragg, G.M. and Snader, K.M. (1991). Taxol: the supply issue. *Cancer cell*, 3(6), 233-235.

Crone, C. (1971). The blood-brain barrier-facts and questions. *In Ion Homeostasis of the brain Munksgaard*, Copenhagen, 52-62.

Davda, J., Labhasetwar, V. (2002). Characterization of nanoparticle uptake by endothelial cells. *Int J Pharm*, 233, 51-59.

Davis, S.S.(2000). Drug delivery systems. *Interdiscip Sci Rev*, 25 (3), 175-83.

Dehauck, M.P., Dehouck, B., Schluep, C., Lemaire, M. and Cecchelli, R.,(2000). Drug transport to the brain: comparison between *in-vitro* and *in-vivo* models of the blood-brain barrier, *Eur J Parm Sci*, 3, 357-365.

Dintaman, J.M., Silverman, J.A.(1999). Inhibition of P-glycoprotein by D-atocopheryl polyethylene glycol 1000 succinate (TPGS). *Pharm Res*,16, 1550 – 1556.

Donehower, R.C., Rowinsky, E.K., Grochow, L.B., Longnecker, S.M., Ettinger, D.S. (1987). Phase I trial of Taxol in patients with advanced cancer. *Cancer Treat Rep*, 71, 1171-1177.

Dong, Y., Feng, S.S.(2004).Methoxy poly(ethylene glycol)-poly(lactide)(MPEG-PLA) nanoparticles for controlled delivery of anticancer drugs. *Biomaterials*, 25, 2843-2849.

Dorr, R.T. (1994). Pharmacology and toxicology of Cremophor EL diluent. *Ann*

Pharmacother, 28, S11-S14.

Drion, N., Leimaire, M., Lefauconnier, J.M., Scherrmann, J.M. (1996). Role of p-glycoprotein in the blood-brain transport of colchicines and vinblastine. *J Neurochem*, 67, 1688 – 1693.

Durieu-Trautmann, O., Foignant-Chaverot, N., Perdomo, J., Gounon, P., Strosberg, A.D., and Couraud, P.O. (1991). Immortalization of brain capillary endothelial cells with maintenance of structural characteristics of the blood-brain barrier endothelium. *In Vitro Cell Dev Biol Anim*, 27, 771-778.

Egleton, R.D., Davis, T.P. (1997). Bioavailability and transport of peptides and peptide drugs into the brain. *Peptides*, 18(9), 1431-9.

Enrlich, P.(1885). Das Sauerstoff-Bedurfnis des Organismus. *Eine Farbenanalytische Studies*, Berlin: hirschwald.

Faranesh, Z. A., Nastley, T.M., Cruz, P. C., Haller, F.M., Laquerriere, P., Leong, W. K., Mcveigh, R. E. (2004). In vitro release of vascular endothelial growth factor from gadolinium-doped biodegradable microspheres. *Magnet Reson Med*, 51, 1265-1271.

Fenart, L., Casanova, A. Dehouck, B., Duhem, C., Slupek, S., Cecchelli,R., Betbeder, D. (1999). Evaluation of effect of charge and lipid coating on ability of 60-nm nanoparticles to cross an in vitro model of the blood-brain barrier. *J Pharmacol Exp Ther*, 291, 3, 1017-1022.

Feng, S.S., Huang, G.F. (2001). Effects of emulsifiers on the controlled release of paclitaxel(Taxol®) from nanospheres of biodegradable polymers. *J Control Release*, 71, 53-69.

Feng, S.S., Shu, C.(2003). Chemotherapeutic engineering:Application and further development of chemical engineering principles for chemotherapy of cancer and other diseases. *Chem Eng Sci*, 58, 4087-4114.

Fjallskog, M.L., Frii, L., Bergh, J. (1993). Is cremophor EL, solvent for paclitaxel, cytotoxic? *Lancet*, 342 (8875), 873.

Foster, K.A., Yazdanian, M., Audus, K.L. (2001). Microparticulate uptake mechanisms of in-vitro cell culture models of the respiratory epithelium. *J Pharm Pharmacol*, 53, 57-66.

Fundaro, A., Cavalli, R., Bargoni, A., Vighetto, D., Zara, G.P., Gasco, M.R. (2000). Non-stealth and stealth solid lipid nanoparticles (SLN) carrying doxorubicin: pharmacokinetics and tissue distribution after i.v. administration to rats. *Pharmacol Res*., 42, 4, 337-343.

Gatmaitan, Z.C., Arias, I.M. (1993). Structure and function of P-glycoprotein in normal liver and small intestine. *Adv pharmacol*, 24, 77-97.

Gelperina, S.E., Khalansky, A.S., Skidan, I.N., Smirnova, Z.S., Bobruskin, A.I., Severin, S.E., Turowski, B., Zanella, F.E., Kreuter, J. (2002). Toxicological studies of

doxorubicin bound to polysorbate 80-coated poly(butyl cyanoacrylate) nanoparticles in healthy rats and rats with intracranial glioblastoma. *Toxicol Lett*, 126, 131-141.

Goldmann, E.(1909). Beitr Klin Chirurg, 64, 192-265.

Govender, T., Stolnik, S., Garnett, C.M., Illum, L., Davis, S.S. (1999). PLGA nanoparticles prepared by nanoprecipitation: drug loading and release studies of a water soluble drug. *J Control Release*, 57, 171-185.

Greenberger, L.M., Williams, S.S. and Horwitz, S.B. (1987). Biosynthesis of heterogeneous forms of multidrug resistance-associated glycoproteins. *J Biol Chem*, 5, 262 (28), 13685-13689.

Gref, R., Minamitake, Y., Perachhia, M.T., Trubetskoy, Torchilin, V., Langer, R.(1994). Biodegradable long-circulating polymeric nanospheres. *Science*, 18, 263 (5153), 1600-3.

Gulyaev, A., Gelperina, S.E., Skidan, I.N., Antropov, A.S., Kivman, G.Y., Kreuter, J. (1999). Significant transport of doxorubicin into the brain with polysorbate 80 coated nanoparticles. *Pharm Res*, 16 , 10, 1564-1569.

Gulyaev, A.E, Gelperina, S.E, Skidan, I.N, Antropov, A.S, Kirman, G.Y, Kreuter, J. (1999). Significant transport of doxorubicin into the brain with polysobate 80-coated nanoparticles. *Pharm Res*, 16 (10), 1564-9.

Horwitz, S.B. (1992). Mechanism of action of Taxol. *Trends Pharmacol Sci*, 13,

134-136.

Huwyler, J., Yang, J. and Pardridge, W.M. (1997). Targeted delivery of daunomycin using immunoliposomes: pharmacokinetics and tissue distribution in the rat. *J Pharmacol Exp Ther*, 282, 1541-1546.

In vitro model of BBB http://www.umu.se/pharm-neuro/inst/Stig.html

Jain, A.R. (2000). The manufacturing techniques of various drug loaded biodegradable poly (lactide-*co*-glycolide) (PLGA) devices. *Biomaterials*, 21, 2475-2490.

Joo, F. (1992). The cerebral microvessels in culture, an update. *J Neurochem*, 58, 1-17.

Kakee, A., Terasaki, T. and Sugiyama, Y. (1996). Brain Efflux index as a novel method of solute analyzing efflux transport at the blood brain barrier. *J Pharmacol Exp Ther*, 277, 1550-1559.

Khin, Y.W., Feng, S. S. (2005). Effects of particle size and surface coating on cellular uptake of polymeric nanoparticles for oral delivery of anticancer drugs. *Biomaterials*, 26, 2713-2722.

Kongshaug, M., Cheng, L.S., Moan, J., Rimington, C. (1991). Interaction of Cremophor-EL with human plasma. *Inter J Biochem,* 23, 473-478.

Koziara, M.J., Lockman, R.P., Allen, D.D., Mumper, J.R. (2004). Paclitaxel

nanoparticles for the potential treatment of brain tumors. *J control release*, 99, 259-269.

Kreuter, J.(1994). Drug targeting with nanoparticles. *Eur J Drug Metab Pharmacokinet*, 19 (3), 253-256.

Kreuter, J.(2001). Nanoparticulate systems for brain delivery of drugs. *Adv Drug Del Rev*, 47, 65-81.

Kreuter, J., Alyautdin, R.N., Kharkevich, D.A., Ivanov, A.A. (1995). Passage of peptides through the blood-brain barrier with colloidal polymer particles (nanoparticles). *Brain Res*, 674, 171-174.

Kreuter, J., Ramge, P., Petrov, V., Hamm, S., Gelperina, E. S., Engelhardt, B., Alyautdin, R., Briesen, H., Begley, J.D.(2003). Direct evidence that polysorbate-80-coaated poly(butylcyanoacrylate) nanoparticles deliver drugs to the CNS via specific mechanisms requiring prior binding of drug to the nanoparticles. *Pharm res*, 20, 3, 409-416.

Kreuter,J., Alyautdin, R.N., Kharkevich, D.A. and Ivanov, A.A. (1995). Passage of peptides through the blood-brain barrier with colloidal polymer particles (nanoparticles). *Brain Res*, 674, 171-174.

Kroll, RA., Neuwelt, EA. (1998). Outwitting the blood-brain barrier for therapeutic purposes: osmotic opening and other means. *Neurosurgery*, 42(5),1083-99, 1099-100.

Kwon, G.S., Kataoka, K. (1995). Block copolymer micelles as long-circulating drug vehicles. *Adv Drug Deliv Rev*, 16, 295-309.

Lee, G., Dallas, S., Hong, M., Bendayan, R. (2001). Drug transporters in the central nervous system: brain barriers and brain parenchyma considerations. *Pharmacol Rev* ,53(4), 569-96.

Leong, K.W., Langer, R. (1987). Polymeric controlled drug delivery. *Adv Drug Deliver Rev*, 1, 199-233.

Lin, R., Ng L.S., Wang, C.H. (2005). In vitro study of anticancer drug doxorubicin in PLGA-based microparticles. *Biomaterials*, 26, 21, 4476-4485.

Lo, E.H., Singhal, A.B., Torchilin, V.P., Abbott, N.J. (2001). Drug Delivery to damaged brain. *Brain Res Rev*, 38(1-2), 140-148.

Lockman, P.R., Mumper, R.J., Khan, M.A., Allen, D.D. (2002). Nanoparticle technopogy for drug delivery across the blood-brain barrier. *Drug Dev Ind Pharm*, 28 (1), 1-13.

Lockman, P.R., Oyewumi, O. M., Koziara, M.J., Roder, E.K., Mumper, J.R., Allen, D.D. (2003). Brain uptake of thiamine-coated nanoparticles. *J control release*, 93, 271-282.

Lockman, R.P., Koziara, M.J., Mumper, J.R., Allen, D.D. (2004). Nanoparticle surface charges alter blood-brain barrier integrity and permeability. *J Drug Target*, 12,

635-641.

Lopes, N.M., Adams, E.G., Pitts, T.W., Bhuyan, B.K. (1993). Cell kill kinetics and cell cycle effects of taxol on human and hamster ovarian cell lines. *Cancer Chemoth Pharm*, 32(3), 235-242.

Lu, W., Tan, Y.Z., Hu, K.l., Jiang, X.G. (2005). Cationic albumin conjugated nanoparticles with its transcytosis ability and little toxicity against blood-brain barrier. *Int J Pharm*, 295, 247-260.

Miller, G. (2002). Breaking down barriers. *Science*, 297, 1116-1118.

Misra Ambikanandan, Ganesh S., Aliasgar Shahwala, Shrenik P. Shah (2003). Drug delivery to the central nervous system: a review. *J Pharm Pharmaceut Sci*, 6(2), 252-273.

Mooradian, D. L., and Diglio, C.A.(1991). Production of a transforming growth factor by RSV-transformed rat cerebral microvasculature endothelial cells, *Tumor Biol*, 12, 171-183.

Morel, S., Terreno, E., Ugazio, E., (1998). NMR relaxometric investigations of solid lipid nanoparticles (SLN) containing gadolinium(III) complexes. *Eur J Pharm Biopharm*, 45 (2), 157-163.

MRI technology website: http://www.mr-tip.com/serv1.php

Mu, L., Feng, S.S.(2002). Vitamin E TPGS used as emulsifier in the solvent

evaporation/ extraction technique for fabrication of polymeric nanopsheres for controlled release of paclitaxel (Taxol®). *J Control Rel*, 80,124-144.

Mu. L., Feng, S.S. (2003). A novel controlled release formulation for anticancer drug paclitaxel (Taxol®): PLGA nanoparticles containing vitamin E TPGS. *J Control Release*, 86(1), 33-48.

Muldoon, L.L., Pagel, M.A., Kroll, R.A., Roman-Goldstein, S., Jones, R.S., Neuwelt, E.A.(1999). A physiological barrier distal to the anatomic blood-brain barrier in a model of transvascular delivery. *AJNR Am J Neuroradiol*, 20, 217-222.

Muruganandam, A., Herx, L. M., Monette, R., Durkin, J.P., and Stran Stranimicrovic, D.B. (1997). Development of immortalized cerebromicrovascular endothelial cell line as an in vitro model of the human blood-brain barrier. *FASEB J* 11, 1187-1197.

Oliver, J.C, Fenart, L., Chauvet, R., Pariat, C., Cecchellia, R., Couet, W.(1999). Indirect evidence that drug brain targeting using polysorbate 80-coated polybutylcyanoacrylate nanoparticles us related to toxicity. *Pharm Res*, 16 (12), 1836-42.

Oncology: treatment and management. Part 2, Cancer treatment. Pharmaceutical representative, November 2002

Oncology channel: http://www.oncologychannel.com/braincancer/

Oyewumi, M.O., Yokel, R.A., Jay, M. (2004).Comparison of cell uptake

biodistribution and tumor retention of folate-coated and PEG-coated gadolinium nanoparticles in tumor-bearing mice. *J Controlled Release*, 95 (3), 613-626

Panchagnula, R. (1998). Pharmaceutical aspects of paclitaxel. *Int J Pharm*, 172 (1-2), 1-15.

Panyam, J., Labhasetwar, V. (2003). Biodegradable nanoparticles for drug and gene delivery to cells and tissue. *Adv Drug Deliv Rev*., 24, 55 (3): 329-347

Panyam, J., Sahoo, S.K., Prabha, S., Bargar, T., Labhasetwar, V. (2003). Fluorescence and electron microscopy probes for cellular and tissue uptake of poly (D,L-lactide-so-glycolide) nanoparticles. *Int J Pharm*, 262, 1-11.

Panyam, J., Zhou, W.Z., Prabha, A., Sahoo, K.S., Labhasetwar, V.A.(2002). Rapid endo-lysosomal escape of poly ($_{DL}$-lactide-*co*-glycolide) nanoparticles: implications for drug and gene delivery. *The FASEB Journal*, 16, 1217-1226.

Pardridge, W.M.(ed). (1998). Introduction to the blood-brain barrier: methodology, biology and pathology. pp. 49-61, Cambridge: University Press

Peltonen, L., Aitta, J., Hyvonen, S., Karjalainen, M., Hirvonen, J. (2004). Improved entrapment efficiency of hydrophilic drug substance during nanoprecipitation of polylactide nanoparticles. *AAPS Pharm Sci Tech*, 5 (1), 16.

Peppas, B. L., Blanchette, O. J. (2004). Nanoparticle and targeted systems for cancer therapy. *Adv drug deliver rev*, 56, 1649-1659.

Ramge, P., Kreuter, J., Lemmer, B.(1999). Circadian phase-dependent antinociceptive reaction in mice after i.v. injection of dalargin-loaded nanoparticles determined by the hot-plate test and the tail-flick test, *Chronobiol. Int.*, 17, 767-777.

Ramge, P., Unger, R.E., Oltrogge, J.B., Begley, D., Briesen von H., Kreuter, J. (2000). Polysorbate 80-coating enhances uptake of polybutylcyanoacrylate (PBCA)-nanoparticles by human, bovine and murine primary brain capillary endothelial cells. *Eur J Neuro*, 12, 1935-1940.

Rapoport, S.I., Ohno, K., Fredericks, W.R., Pettigrew, K.D.(1978). Regional cerebrovascular permeability to [^{14}C] sucrose after osmotic opening of the blood-brain barrier. *Brain Res*, 150 (3), 653-657.

Ratain, M.J., Schilsky, R.L., Conley, B.A., Egorin, M. J. (1990). Pharmacodynamics in cancer therapy. *J Clin Oncol*, 8(10), 1739-1753.

Reese, T.S., Feder, N., Brightman, M.W. (1970). Electron Microscopic Study of the Blood-Brain and Blood-Cerebrospinal Fluid Barriers with Microperoxidase. *Am Assoc Neuropath*, 137-138.

Reese, T.S., Karnovsky, M.J. (1967). Fine structural localization of a blood-brain barrier to exogenous peroxidase. *J Cell Biol*. 34, 207-217.

Roy, S.N. and Horwits, S.B. (1985). A phosphoglycoprotein associated with taxol resistance in J774.2 cells. *Cancer Res*, 45, 8, 3856-3863.

Runge, V.M. (2000). Safety of approved MR contrast media for intravenous injection. *J Magn Reson Imag*, 12, 2, 205-213.

Runge, V.M. (2001). A review of contrast media research in 1999-2000. *Invest Radiol*, 36(2), 123-130.

Runge, V.M., Muroff, L.R., Wells, J.W. (1997). Principles of contrast enhancement in the evaluation of brain diseases: an overview. *J Magn Reson Imag*, 7 (1), 5-13.

Sahoo, S., Panyam, J., Prabha, S., Labhasetwar, V. (2002). Residual polyvinyl alcohol associated with poly(D,L-lactide-co-glycolide) nanoparticles affects their physical properties and cellular uptake. *J Control Release*, 82, 105-114.

Sanovich, E., Bartis, R.T., Friden, P.M., Dean, R.L., Le, H.Q., Brightman, M.W. (1995). Pathway across blood-brain barrier opened by the bradykinin agonist, RMP-7. *Brain Res*., 705 (1-2), 125-135.

Schmiedl, U., Sievers, R.E., Brasch, R.C., Wolfe, C.L., Chew, W.M., Ogan, M.D., Engeseth, H., Lipton, M.J., Moseley, M.E. (1989). Acute myocardial ischemia and reperfusion: MR imaging with albumin-Gd-DTPA. *Radiology*, 170, 351-356.

Schroder, U., Sabel, B.A. (1996). Nanoparticles, a drug carrier system to pass the blood-brain barrier, permitcentral analgesic effects of i.v. dalargin injections. *Brain Res*, 710, 121-124.

Schroeder, U., Sommerfeld, P., Sabel, B.A.(1998). Efficacy of oral dalargin-loaded

nanoparticle delivery across the blood brain. *Peptides*, 19(4), 777-80.

Shikata, F., Tokumitsu, H., Ichikawa, H. (2002). In vitro cellular accumulation of gadolinium incorporated into chitosan nanoparticles designed for neutron-capture therapy of cancers. *Euro J Pharm Biopharm*, 53, 1, 57-63.

Singla, K., Garg, A., Aggarwal, D. (2002). Paclitaxel and its formulations, *Int J Pharm*, 235, 179-192.

Smith, Q.R.(1996). Brain perfusion systems for studies of drug uptake and metabolism in the central nervous system. *Pharm Biotechnol*, 8, 285-307

Stolnik, S., Garnett, M. C., Davies, M. C., Illum, L., Bousta, M., Vert, M., Davis, S. S. (1995). The colloidal properties of surfactant-free biodegradable nanospheres from poly(ß-malic acid-*co*-benzyl malate)s and poly(lactic acid-*co*-glycolide). *Colloids Surfaces A Physicochem Eng Aspects*, 97,235-245.

Suh, H., Jeong, B., Liu, F., Kim, W.S. (1998). Cellular uptake study of biodegradable nanoparticles in vascular smooth muscle cells. *Pharm Res*, 15 (9), 1495-1498.

Sun, W., Xie, C., Wang, H., Hu, Y. (2004). Specific role of polysorbate 80 coating on the targeting of nanoparticles to the brain. *Biomaterials*, 25, 3065-3071.

Takasato, Y., Rapoport, S.I., and Smith, Q.R. (1984). An *in situ* brain perfusion technique to study cerebrovascular transport in the rat. *Am J Physiol*, 247, H484-H493.

Tamai, L, Tsuji, (2000). Transporter-mediated permeation of drugs across the blood-brain barrier. *A J Pharm Sci*, 89(11), 1371-1388.

Teifel, M., and Friedl, P. (1996). Establishment of the permanent microvascular endothelial cell line PBMEC/C1-2 from porcine brains. *Exp Cell Res*, 228, 50-57.

Torchilin, V.P., Papisov, M.I.(1994). Hypothesis: why do polyethylene glycol-coated liposomes circulate so long? *J Liposomes Res*, 4, 725-739.

Uhrich, E.K., Cannizzaro, M.S., Langer, S.R., Shakesheff, M. K. (1999). Polymeric systems for controlled drug release. *Chem Rev*, 99, 3181-3198.

Verma, A.K., Sachin, K., Saxena, A., Bohidar, H.B. (2005). Release kinetics from bio-polymeric nanoparticles encapsulating protein synthsis inhibitor- cycloheximide, for possible therapeutic applications. *Curr Pharm Biotechnol*, 6(2), 121-130.

Wagenaar, B.W., Muller, B.W.(1994). Piroxicam release from spry-dried biodegradable microspheres. *Biomaterials*, 15(1), 49-54.

Wang, S.C., Wikstrom, M.G., White, D.L., Klaveness, J., Holtz, E., Rongved, P., Moseley, M.E., Brasch, R.C. (1990). Evaluation of Gd-DTPA labeled dextran as an intravascular MR contrast agent: imaging characteristics in normal rat tissues. *Radiology*, 175, 483-488.

Wang,Y., and Welty, D.F.(1996). The simultaneous estimation of the influx and efflux blood-brain barrier permeabilities of gabapentin using a microdialysis-

pharmacokinetic approach. *Pharm Res*, 13, 398-403.

Wani, M.C., Taylor, H.L., Wall, M.E., Coggon, P., Mcphail, A.T. (1971). Plant antitumor agents, VI: the isolation and structure of taxol, a novel antileukemic and antitumor agent from taxus brevifolia. *J Ame Chem Society*, 93, 2325-2327.

Watanabe, T., Ichikawa, H., Fukumori, Y. (2002). Tumor accumulation of gadolinium in lipid-nanoparticles intravenously injected for neutron-capture therapy of cancer. *Euro J Pharm Biopharm*, 54, 2, 119-124.

Web definitions for cancer. http://en.wikipedia.org/wiki/Cancer

Weiler-Guttler, H., Zinke, H,, Mockel, B., Frey, A., Gassen, H.G. (1989). cDNA cloning and sequence analysis of the glucose transporter from porcine blood-brain barrier. *Biol Chem Hoppe Seyler*, 370(5), 467-473.

Weiss, R.B., Donehower, R.C., Wiernik, P.H., Ohnuma, T., Gralla, R.J., Trump, D.L., Baker, R., Vanecho, D.A., VonHoff, D.D., Leyland-Jones, B. (1990). Hypersensitivity reactions from taxol. *J Clin Oncol*, 8 (7), 1263-1268

Wijsman, J.A., and Shievers, R.R. (1998). Immortalized mouse brain endothelial cells are ultrastructurally similar to endothelial cells and respond to astrocyte-conditioned medium. *In vitro Cell Dev Biol Anim*, 34, 777-784.

PUBLICATION LIST

1. Internationally Refereed Journal Paper

1. *In vitro* evaluation of paclitaxel loaded poly ($_{D,L}$-lactide-co-glucolide) (PLGA) nanoparticles to cross the blood brain barrier with novel natural surfactant (in preparation)

2. *In vitro* evaluation of MRI contrast agent Gadolinium-DTPA encapsulated nanoparticles for potential brain imaging (in preparation)

2. International Conference papers

1. Yu Q., Chen L., Feng SS., Nanoparticles for Chemotherapy across the Blood Brain Barrier- Effects of Emulsifier and Particle Size. World Conference on Dosing of Antiinfectives, September 2004, Nurnberg, Germany (invited presentation)

2. Chen Lirong, Yu Qianru, Wang Junping, Nanoparticles of biodegradable polymers to cross the blood brain barrier. 1st Nano-Engineering and Nano-Science Congress 2004, July 2004, Singapore

3. Chen L., Yu Q., Feng SS, Surface coating effects on nanoparticles of biodegradable polymers to cross the blood brain barrier. World Conference on Dosing of Antiinfectives, September 2004, Nurnberg, Germany